Public-data File 86-2

GEOLOGY OF THE GODDARD HOT SPRINGS AREA, BARANOF ISLAND, SOUTHEASTERN ALASKA

by

R.R. Reifenstuhl

Alaska Division of
Geological and Geophysical Surveys

1986

3700 Airport Way
Fairbanks, Alaska 99709

ABSTRACT

Detailed geologic investigation of 250 km2 about 25 km south of Sitka, Alaska yields three major lithologic units: (1) the Upper Cretaceous Sitka Graywacke, (2) the middle Eocene Crawfish Inlet pluton, and (3) the 4-km-wide biotite and hornblende hornfels contact metamorphic aureole. The clastic rocks are inner submarine fan turbidity current deposits with lesser lower slope deposits that have been imbricately thrust faulted in a subduction zone. The provenance terrane is a volcano-plutonic complex. The reverse-zoned, hornblende-bearing pluton contains three gradational facies: (1) the centrally located tonalite, (2) the granodiorite, and (3) the primary white mica-bearing, locally peraluminous border facies. Biotite and hornblende separates yield K-Ar dates of 48.0 $\pm$ 1.4 and 48.3 $\pm$ 1.4 m.y. respectively. Four uncontaminated samples were analyzed for Rb, Sr and Sr isotope composition. Initial 87Sr/86Sr ratios, calculated using the 48.0 m.y. age, range from 0.70464 to 0.70527. Minimum depth of crystallization is about 6 km. Previously, this pluton was included in the Sanak-Baranof belt of anatectic, early Tertiary plutons that intrude the Chugach terrane along the Gulf of Alaska. However, new whole rock-major oxide, point count, and field data indicate a non-anatectic paragenesis and other important differences from descriptions of plutons in this belt, and preclude inclusion of the Crawfish Inlet pluton.

The Goddard Hot Springs geothermal system has a subsurface reservoir temperature of about 145°C and, at least in part, a high-altitude, heavy isotope-depleted recharge source. Total flow of the four surface seeps is 70 liters/minute and surface temperatures range from 65.3 to 50.1°C. Fluid geochemistry is characterized by: 1) total dissolved solids - 5000 ppm, 2) Na - 1300 ppm, 3) Cl - 2720 ppm, and 4) specific conductance - 8000 umhos/cm at 25°C. The Goddard system is a liquid-dominated, warm water system with thermal transfer of the water-dominated, convective heat-type. Geothermal fluids are reheated during deep circulation in a region of high to normal regional geothermal gradient: 42 to 25°C/km.

TABLE OF CONTENTS

	page
ABSTRACT	1
TABLE OF CONTENTS	2
LIST OF FIGURES	4
LIST OF TABLES	6
INTRODUCTION	7
Geography	7
PREVIOUS INVESTIGATIONS	10
REGIONAL STRUCTURAL SETTING	12
THE SITKA GRAYWACKE	14
Introduction	14
Age and correlations	14
Structure	14
Lithology	17
Rock fragment petrography	17
Turbidite facies and fan associations	19
Application of facies model to Goddard area	19
Facies A and B - Massive sandstone	21
Facies E - Overbank turbidites	21
Facies C - Classic proximal turbidites	21
Facies F - Chaotic deposits	22
Facies G - Hemipelagic shale	22
Facies associations and submarine fan environment	22
Tectonic setting	23
THE CRAWFISH INLET PLUTON	24
Introduction	24
Plutonic rock facies and modal mineralogy	24
Goddard area plutonic rock facies	24
The tonalite facies	24
Mineralogy of the tonalite facies	31

page

The granodiorite facies 32

Mineralogy of the granodiorite facies 32

The border facies 33

Mineralogy of the border facies 34

Major oxide chemistry 35
Depth of crystallization 41
Pluton consanguinity 41
Rubidium and strontium isotopes 41
Conclusions 46

CONTACT METAMORPHIC ROCKS 51

Introduction 51
Biotite zone - outer aureole 51
Hornblende hornfels facies - inner aureole 51
Pressure-temperature restrictions 53

HYPABYSSAL DIKES 54

Felsic dikes 54
Hornblende diabase dikes 54
Alkali-olivine diabase dikes 56
Dike chemistry 56

GODDARD HOT SPRINGS 58

Introduction 58
Fluid geochemistry 58
Geothermometers 62
Geochemical constraints on hot springs water source 62
Isotope geochemistry 63
Interpretation 66

SUMMARY OF CONCLUSIONS 68

REFERENCES CITED 71

APPENDIX 1 - WHOLE ROCK MAJOR OXIDE AND CIPW NORM DATA FOR SOME ROCKS OF THE GODDARD AREA 76

APPENDIX 2 - GEOLOGIC MAP OF THE GODDARD HOT SPRINGS AREA In pocket

LIST OF FIGURES

Figure		Page
1	Goddard area location map	8
2	Goddard area, Baranof Island and adjacent Islands	9
3	Stereographic plot of bedding plane attitudes from the Sitka Graywacke	15
4	Deformation of accreted material in a subduction zone	16
5	FeO*/MgO versus SiO2 for some mafic dikes and greenstones	18
6	Environmental model and stratigraphic sections representative of turbidite facies	20
7	Location map of Sanak-Baranof Tertiary intrusive belt	26
8	IUGS plutonic rock classification diagram for some Goddard area rocks	28
9	Contoured modal mineralogy for plutonic rocks of the Goddard area	29
10	Plutonic rock facies of the northwestern portion of the Crawfish Inlet pluton	30
11	Whole-rock, major oxide value traverse into the Crawfish Inlet pluton	36
12	Plot of normative albite, anorthite and orthoclase for 23 plutonic rocks from the northwestern portion of the Crawfish Inlet pluton	38
13	Al2O3 versus (CaO+Na2O+K2O) in molecular proportions for 23 rocks from the northwestern portion of the Crawfish Inlet pluton	39
14	Al2O3 versus (CaO+Na2O+K2O) in molecular proportions for some greenstones, hornfels and xenoliths from the Goddard area	40
15	Plot of normative albite, orthoclase and quartz for an aplite dike of the Crawfish Inlet pluton	42
16	Differentiation index versus normative plagioclase composition for some igneous rocks of the Goddard area	43
17	AFM variation diagram for 23 rocks from the northwestern portion of the Crawfish Inlet pluton	44
18	Values of 87Sr/86Sr and 87Rb/86Sr for the Crawfish Inlet pluton plotted on an isochron diagram	47

Figure		Page
19	Compositional range of the Sanak-Baranof pluton belt and the Crawfish Inlet pluton	50
20	Bulk composition of Sitka Graywacke plotted on the metamorphic AFM projection plane	52
21	Stereographic projection of attitudes of 35 hypabyssal dikes from the Goddard area	55
22	AFM variation diagram for some greenstones and mafic dikes from the Goddard area	57
23	Deuterium and oxygen-18 compositions of geothermal fluid from the Goddard Hot Springs and area waters	64

LIST OF TABLES

Table		Page
1	Analytical data for K-Ar age determinations	25
2	Rubidium and strontium isotopic data for the Crawfish Inlet pluton	45
3	Geochemical data on Goddard Hot Springs	59
4	Geochemical data on some Goddard area cold water streams	60
5	Geochemical and isotopic data from previous workers for Goddard Hot Springs and area cold stream	61

INTRODUCTION

Goddard Hot Springs (lat. 56°50'07"N., long. 135°22'30"W.) is 24 km south of Sitka, Alaska, on the west central coast of Baranof Island and is centrally located within the region mapped (figure 1). The Goddard area is located in the eastern portion of the D-5 and the western portion of the D-4 Port Alexander quadrangles.

This report includes: 1) a detailed (1:40,000 scale) geologic map, 2) assignment of three gradational facies to the Crawfish Inlet pluton on the basis of field mapping, modal mineralogy, xenolith abundance and major oxide chemistry, 3) data supporting anatexis along the margin of the Crawfish Inlet pluton, 4) pressure-temperature estimates for pluton emplacement, 5) Rb/Sr isotopic data, 6) interpretation of the Sitka Graywacke turbidite sequence in light of the Mutti and Ricci Lucchi (1972) submarine fan model, 7) a brief discussion of sandstone petrography, and 8) evaluation of the Goddard Hot Springs geothermal system.

Geography

Baranof Island is one of the large islands of southeastern Alaska's Alexander Archipelago a 450 km long by 130 km wide area composed of numerous islands. Four other large islands in the Archipelago, and their geographic relationship to Baranof Island are: Chichagof - to the north, Admiralty - to the northeast, and Kuiu and Kupreanof Islands to the east (figure 2).

The entire area of investigation lies within the Tongass National Forest except nearly 30 acres surrounding the hot springs which belong to the City and Borough of Sitka. The hot springs issue at elevations of between 15 m and 24 m above mean high tide, and lie 120 m to 140 m inland from tidewater.

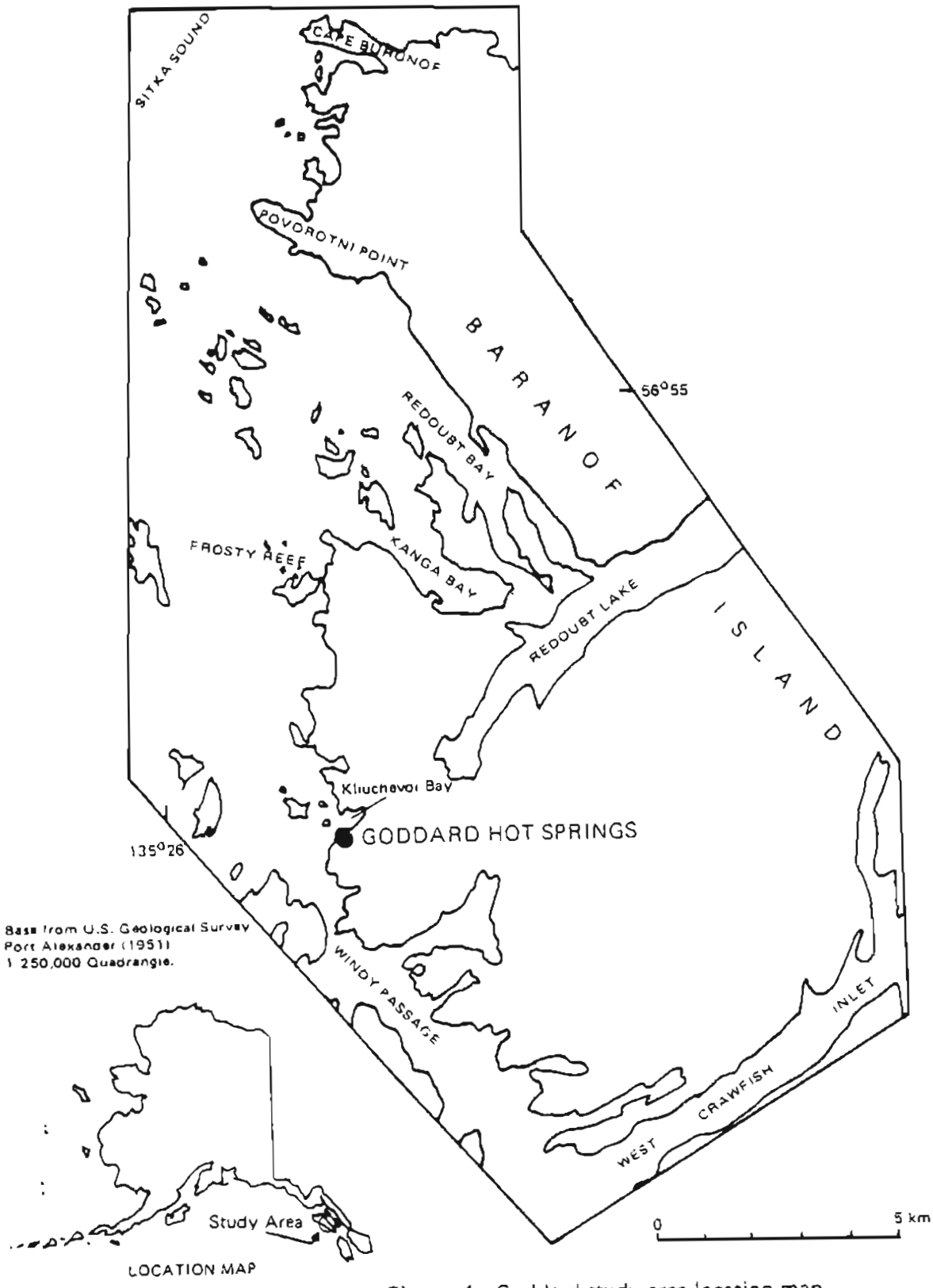

Figure 1. Goddard study area location map.

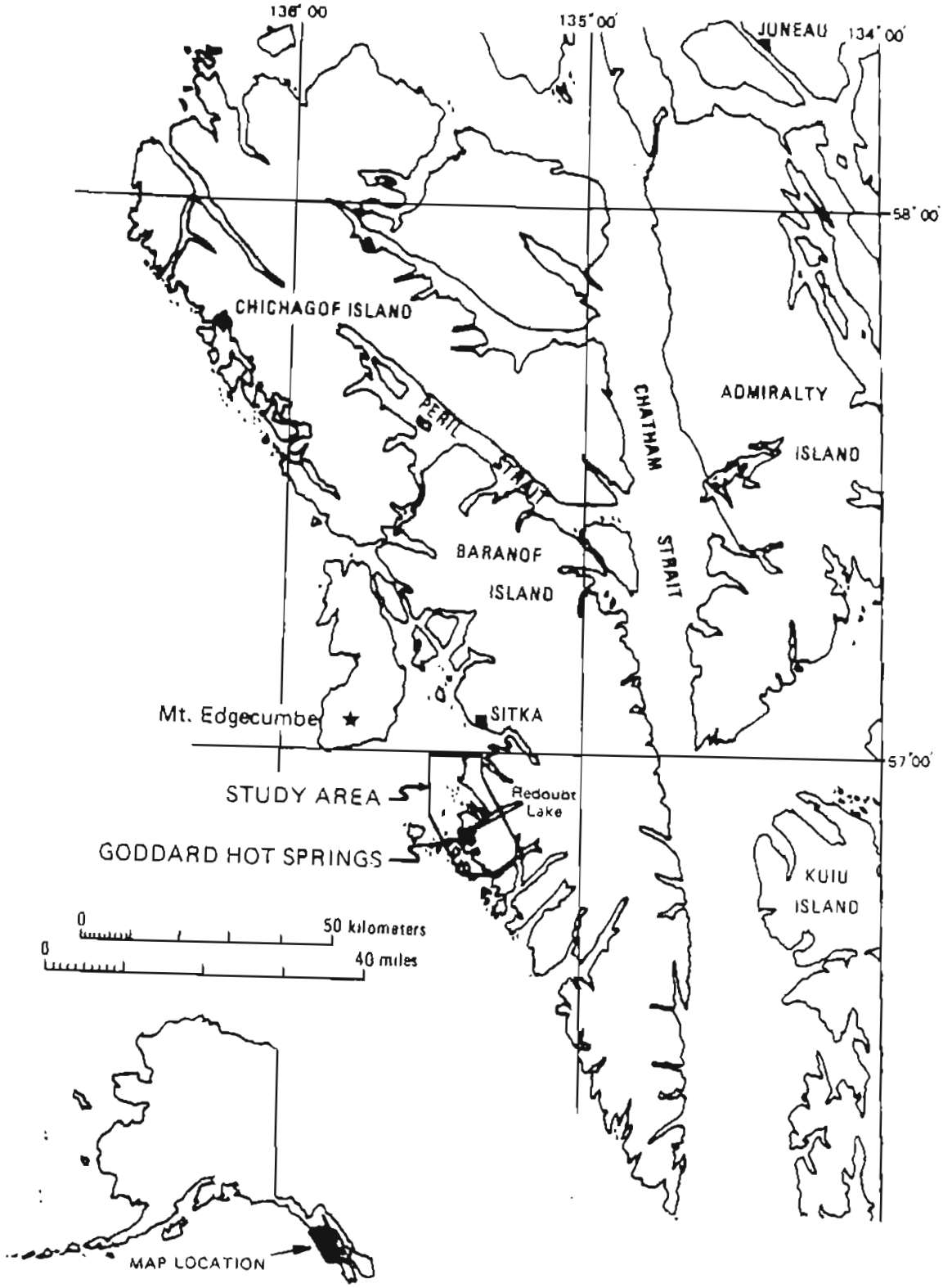

Figure 2. Goddard study area, Baranof Island and adjacent islands.

PREVIOUS INVESTIGATIONS

In 1917 Goddard Hot Springs (then known as the Sitka Hot Springs) were discussed in some detail by G.A. Waring (Waring, 1917). He wrote that, among Alaska's mineral springs, these were the earliest known to white men. Waring found four spring sites, measured flows from 38 liters/minute to one showing no appreciable flow, and recorded temperatures ranging from 35 to 65°C. The hot water was determined to be a mineral-rich sodium chloride solution in which chloride constituted more than half of the total dissolved solids.

In the early 1920's, Dr. Goddard bought the springs and surroundingland, built a three story sanitarium, and the springs became known as the Goddard Hot Springs. During this time the hot water was used to heat the sanitarium and several smaller buildings, including a greenhouse. Raised in 1954, currently only foundations and iron pipes remain as evidence of the buildings. At present, the only permanent structures in the springs vicinity are two small wooden bath houses.

Hicks and Shofnos (1965) discussed the Sitka vicinity and Redoubt Lake (a relic fiord centrally located within the study area). They have shown an isostatic rebound rate of about 0.25 cm per year due, at least in part, to the off-loading of the Pleistocene glaciers. Hicks and Shofnos concluded that the lake was open to the ocean less than 800 years ago on the basis of: (1) a 0.25 cm per year rate of uplift, (2) the lake's saline nature below 100 m, and (3) the lake's present elevation of 0.6 m above maximum high tide. The unusual deep zone of salinity (two-thirds as saline as sea water) within the otherwise fresh water of Redoubt Lake is characteristic of a meromictic lake and makes it one of the largest lakes of this type documented in North America (McCoy, 1977).

Loney and others (1975), summarized the geology of the hot springs region in a reconnaissance geologic report of Chichagof, Baranof, and Kruzof Islands. They recognized the major rock units within the Goddard area to be: the Sitka Graywacke, the Crawfish Inlet pluton, and hornfels associated with the pluton.

The most recent work dealing with the hot springs was the analysis of the water chemistry (Bliss, 1983). An extensive chemical species list for the Goddard Springs thermal fluids, and other hot springs in Alaska was presented in tabular form.

REGIONAL STRUCTURAL SETTING

Southeastern Alaska is a structurally complex area cut by numerous high angle faults. The most notable of these are the 190 km-long Fairweather-Queen Charlotte fault system offshore of Chichagof and Baranof Islands and the 400 km-long Chatham Strait fault (juxtaposing Chichagof and Baranof Islands and Admiralty and Kuiu Islands to the east). The Fairweather-Queen Charlotte system is a right-lateral strike slip fault between the Pacific and the North America plates that dips steeply to the northeast (Page, 1973). The Pacific plate is moving northwestward approximately 6 cm per year and has a minor component of underthrusting relative to the North American plate (von Huene and others, 1977). Movement along the fault has taken place during Tertiary and Quaternary time (Gehrels and others, 1983). Recent displacements along the fault were documented during the 1958 earthquake when movement consisted of an upward displacement of 1.1 m on the west side and a left-lateral slip of 0.7 m (Tocher and Miller, 1959). Though the sense of movement along the fault in the 1958 event was left lateral, overall, the Fairweather-Queen Charlotte system is still considered to be right lateral (von Huene and others, 1977; Tocher and Miller, 1959; Gehrels and others, 1983).

The Chatham Strait fault, also a high angle and right-lateral strike-slip fault, has had a horizontal movement of 190 km and vertical west-side-up displacements of over 1.6 km (Loney and others, 1975). Twenhofel and Sainsbury (1958) suggest that the age of much of the displacement along the fault is Cretaceous or younger, and that the fault may be currently active. Gehrels and others (1983) have suggested that the Chatham Strait fault and related fault systems may have approximately 350 km of post-Devonian right-lateral displacement.

A group of faults, considered by Loney and others (1975) to be less important than the Chatham Strait or Fairweater faults, was named the Tenakee fault system. These NW-and NNW-trending faults on northern Chichagof Island include: the Freshwater Bay fault, the Indian River fault, the Sitkoh Bay fault, and a large number of minor faults. Right-lateral movement of several kilometers and vertical displacement of less than one kilometer (SW side up) before the Tertiary intrusive episode has been inferred for this system (Loney and others, 1975).

The highly faulted nature of southeastern Alaska in general was documented by Twenhofel and Sainsbury (1958). In their study prominent linear features interpreted as faults were plotted from aerial photos of southeastern Alaska yielding one well defined system trending northwestward and three ill-defined systems trending northerly, northeasterly and easterly. Twenhofel and Sainsbury (1958) note that most of the hot springs of southeastern Alaska occur on conspicuous faults.

THE SITKA GRAYWACKE

Introduction

The Sitka Graywacke crops out along the west coasts of Baranof, Chichagof, and Kruzof Islands (Loney and others, 1975). These flyschoid deposits are marine turbidites of probable Late Cretaceous age, on the basis of continuity with the Valdez Group (Plafker and others, 1977). The Sitka Graywacke is part of the Chugach terrane (Berg and others, 1978) of southern Alaska which extends for approximately 2000 km along the margin of the Gulf of Alaska. Correlative stratigraphy on Chichagof Island was recognized as a Cretaceous subduction complex by Decker (1980).

Structure

The Sitka Graywacke is the main rock unit in the northern Goddard area, extending from Cape Barunof 10 km south to its contact with the Tertiary age Crawfish Inlet pluton. The interbedded graywacke and shale sequence strikes N 70 W, on the average, and dips steeply (figure 3). Stratigraphic tops are to the northeast regardless of whether the beds are up-right or overturned due to imbricate thrusting (Seely and others, 1974). In the trench slope model of Seely and others (1974) tectonic stacking is caused by underthrusting of the oceanic plate beneath the overlying sediments (figure 4) with thrusts and folds as the primary structures. Accretion yields imbricately thrust-faulted, progressively older trench sediments landward over-time. In the Goddard area Sitka Graywacke imbricate thrusting has juxtaposed one tectonic block against another during subduction. Since the strata are not isoclinally folded, stratigraphic tops typically have a similiar orientation. In the Goddard area Sitka Graywacke stratigraphic tops are to the

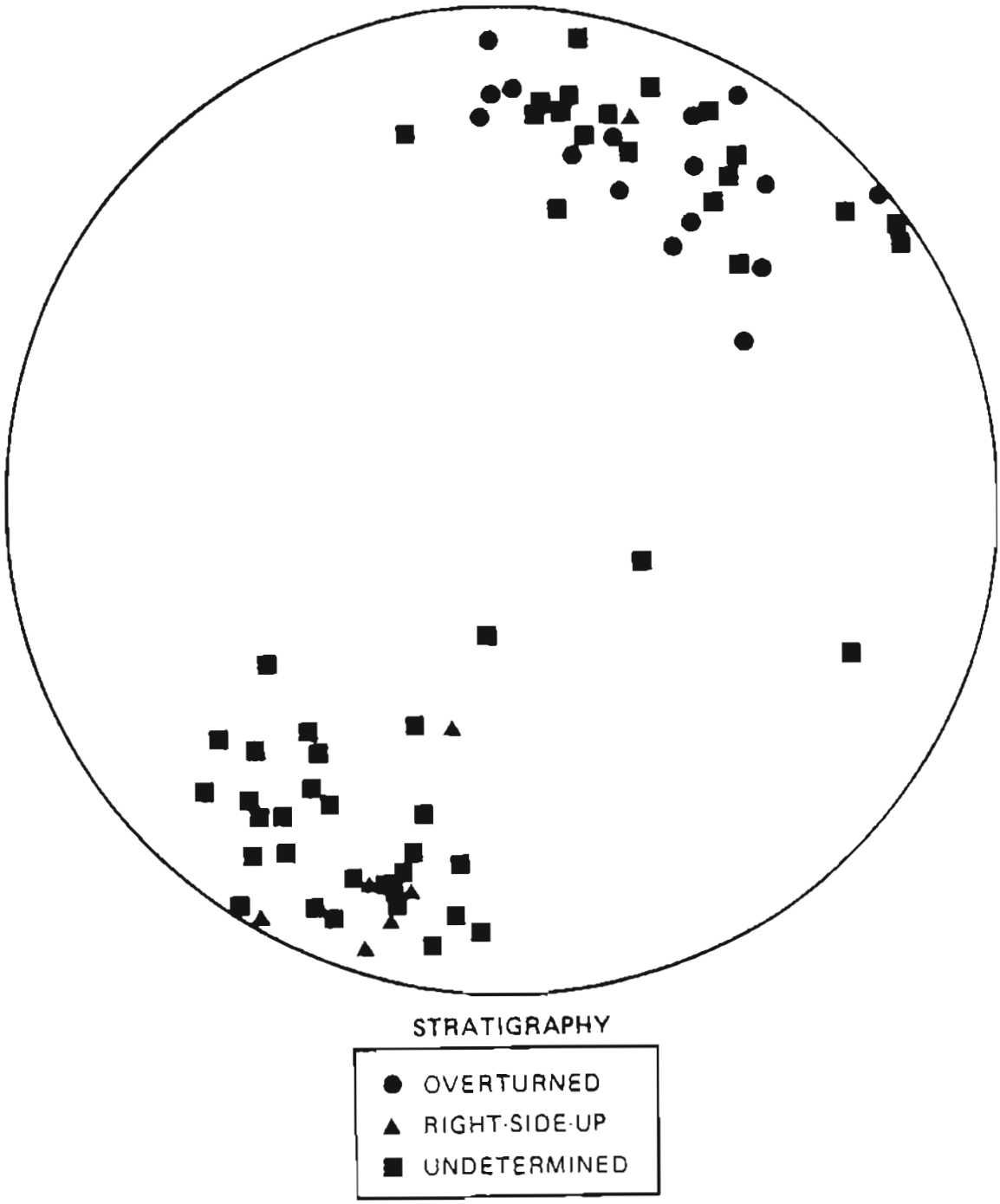

Figure 3. Lower hemisphere, stereographic plot of 74 bedding plane attitudes of the Sitka Graywacke from the Goddard area. Stratigraphic tops determined by repeated graded bedding.

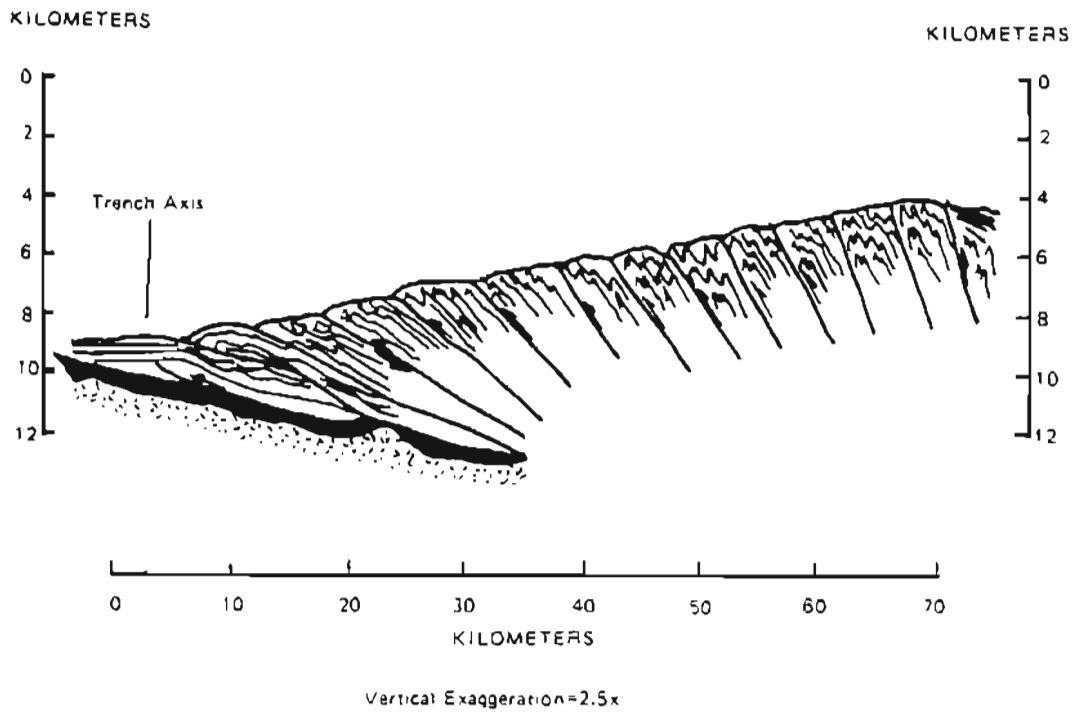

Figure 4. Deformation of accreted material in a subduction zone. Accretion occurs in fold or thrust packets. From Karig and Sharman (1975).

northeast. Tectonic block thickness in the Goddard area ranges from hundreds of meters to kilometers. Prominent joint sets are at high angles to the bedding.

Lithology

The Sitka Graywacke is a flysch-like sequence of dark- to medium-gray, massive to thin-bedded, coarse- to fine-grained lithic sandstone with minor shale and conglomerate (clasts to 10 cm) and tectonic blocks of volcanic rocks. Thin section evaluation indicates that the graywacke is a poorly sorted, angular to sub-angular feldspathic litharenite to lithic arkose (Folk, 1974). Sandstone matrix (approximately 10 percent) consists mostly of argillaceous material.

Volcanic rocks in the Goddard area Sitka Graywacke occur at Kanga Point and Kanga Bay within the biotite hornfels zone. The light green, aphanitic, discontinuous bodies are areally associated with mudstone. These volcanic rock - mudstone sequences have undergone soft sediment deformation obscuring original depositional relationships. Within 2 km of the pluton contact, the volcanic rocks are hornfelsed to albite-epidote facies metamorphism and contain up to 20 percent actinolite. Less metamorphosed volcanic rocks plotted on a FeO (total Fe as FeO=0.9Fe2O3+FeO)/MgO versus SiO2 diagram indicate tholeiitic affinities (figure 5). One sample contains 62 percent SiO2 and is probably theresult of secondary silicification.

Rock fragment petrography

Clast composition estimates on coarse-grained sandstones indicate 25 percent quartz, 25 percent volcanic rock fragments, 20 percent plagioclase, 12 percent shale, slate or phyllite, 8 percent potassium feldspar, 3 percent hornblende, 3 percent biotite, and

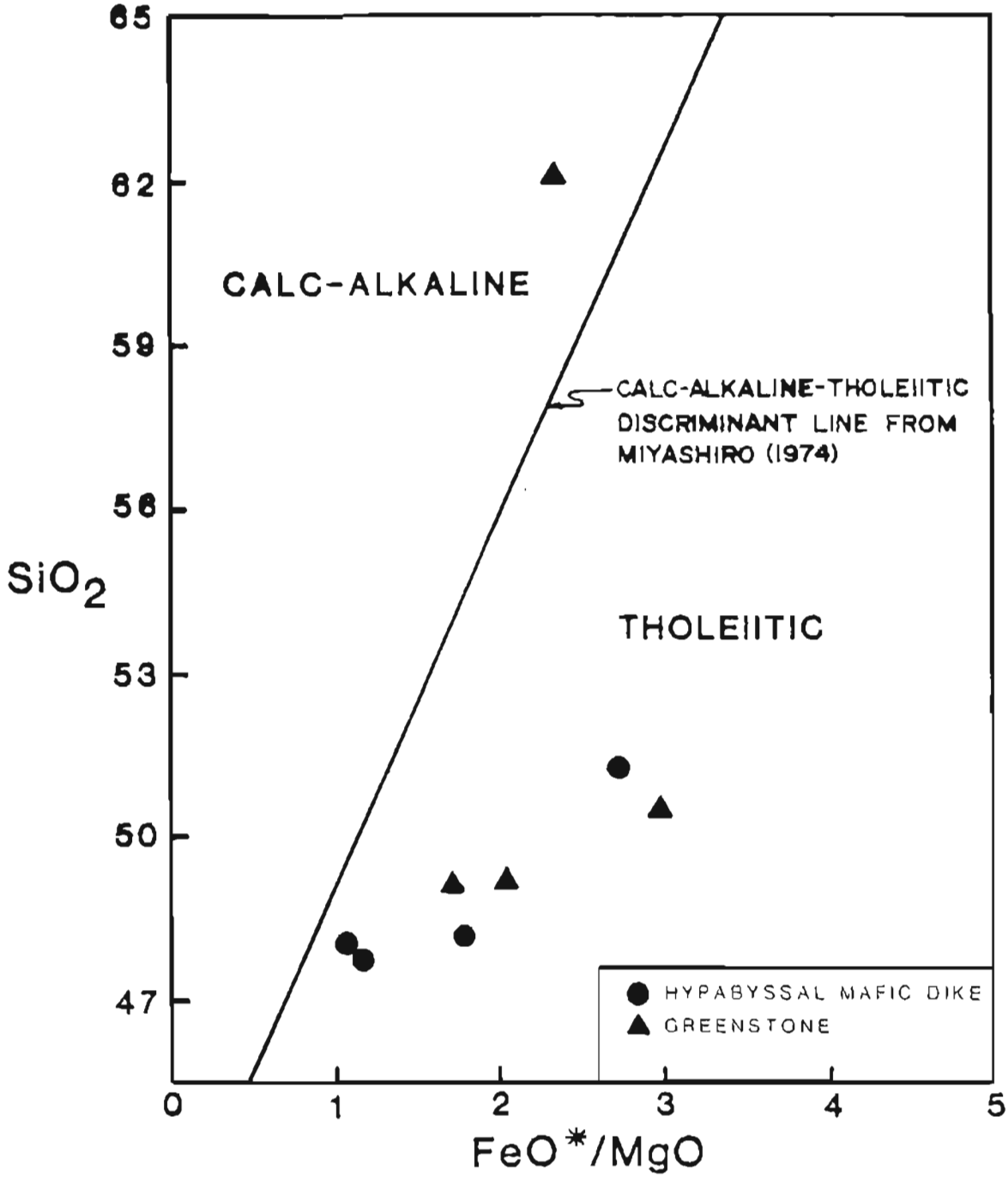

Figure 5. FeO* (total Fe as FeO : $0.9Fe_2O_3$+FeO)/MgO ratio versus SiO_2 in Goddard area mafic dikes and greenstones.

minor white mica, myrmekite and chert. This suite of fragments suggests a plutonic source on the basis of the myrmekite, a volcanic source on the basis of the volcanic rock fragments, and a low grade metamorphic terrane on thebasis of shale or slate. However, the slate and shale clasts are predominantly intraformational rip-ups. The provenence terrane is here interpreted as a volcano-plutonic complex with associated low grade country rocks. Other workers (Moore, 1973; Decker, 1980; Zuffa and others, 1980) have made similiar interpretations based on far more detailed sandstone petrography from elsewhere in the Chugach terrane.

Turbidite facies and fan associations

The facies nomenclature used here is that of Mutti and Ricci Lucchi (1972) and Walker and Mutti (1973). Each of the seven submarine fan facies (A through G) discussed below represents one or more depositional processes. Facies associations are in turn interpreted in terms of depositional environments: 1) slope association, 2) submarine fan association (which is further subdivided into the inner, middle and outer fan associations), and 3) basin plain association (figure 6).

Application of Facies Model to Goddard Area Sitka Graywacke

Facies A, B, C, E, F, and G are represented in the Goddard area Sitka Graywacke, with Facies A+B+F constituting 80 percent of area rocks. These rocks are extremely variable in grain size and bedding thickness. In general, the clasts range from very fine grained sand to cobble size. Bed thickness ranges from less than 1 cm to more than 10 m.

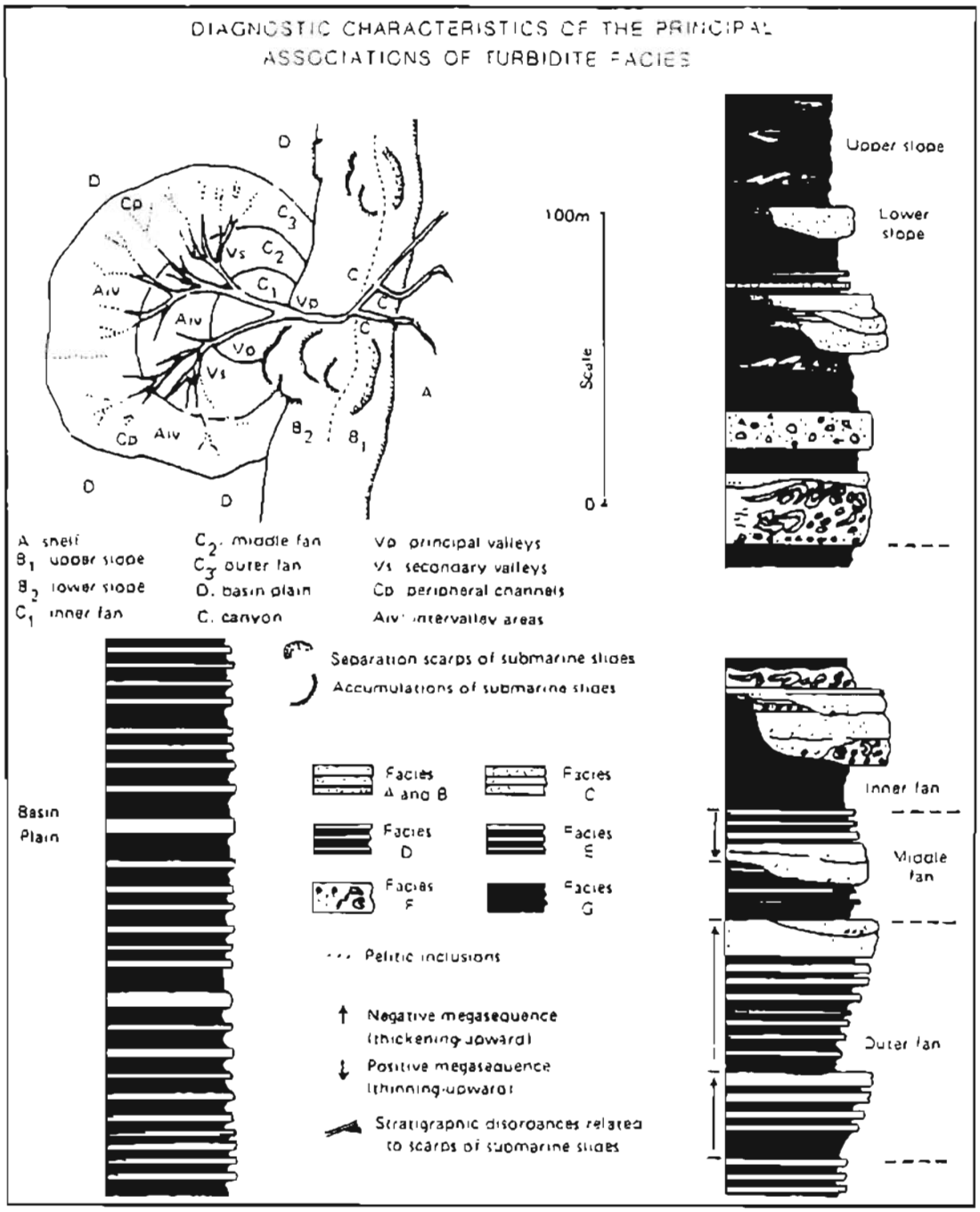

Figure 6. Environmental model and stratigraphic sections representative of the principal associations of turbidite facies. From Mutti and Ricci Lucchi (1972).

Facies A and B - Massive sandstone

The sandstone/shale ratio is typically very high (greater than 10/1) and massive sandstone beds 15 m thick are fairly common. These thick sandstone beds typically are a result of amalgamation, a process whereby successive turbidites are welded together without interbedded shales. This feature is typical of Facies A or B. Massive, medium- to coarse-grained sandstone with minor interbedded shale is the predominant rock type in the Taigud Islands, Povorotni Point, Mielkoi Cove, and Kita Island areas. I interpret these rocks to be Facies B and A deposits with lesser amounts of overbank deposits of Facies E. About 70 percent of the Goddard area rocks are classified as Facies B and A deposits.

Facies E - Overbank turbidites

Facies E deposits commonly have sharp bases and tops. About 5 percent of the Goddard area rocks are classified as Facies E deposits.

Facies C - Classic proximal turbidites

The more "classical" turbidites, with a complete Bouma sequence are also present and locally the divisions are traceable for tens of meters. Outcrops at Cape Burunof and Pirate Cove show well developed repetitions of complete Bouma sequences 40 cm thick with sandstone to shale ratios of greater than 30 to 1. The complete Bouma sequence with lateral continuity are characteristics of Facies C. Less than 5 percent of the Goddard area rocks are here classified as Facies C deposits.

Facies F - Chaotic deposits

Chaotic deposits generally occur in minor amounts in the Sitka Graywacke of the Goddard area but at the head of Redoubt Bay they crop out extensively. Here, chaotically intermixed sandstone and argillite melange indicate pre-lithification to syn-lithifacation mixing. Chaotic deposits of this type are typical of Facies F sedimentation. Locally, folded strata bound above and below by planar strata indicate that these chaotic deposits definitely formed by down-slope movement. Where evidence of gravity-induced slumping and sliding is documented, deposits of Facies F may be assigned to the F1 subdivision of Decker (1980). Facies F deposits constitute approximately 10 percent of the Goddard area rocks.

Facies G - Hemipelagic shale

Massive shale beds (up to 20 m thick) crop out at Frosty Reef and are interpreted as hemipelagic sediments of Facies G. Hemipelagic sediments commonly occur in small amounts throughout the Goddard area but the largest continuous section occurs at Frosty Reef. Facies G constitutes about 10 percent of the rocks mapped.

Facies associations and submarine fan environment

Facies associations (figure 6) of the Goddard area Sitka Graywacke indicate predominantly an inner submarine fan environment and to a lesser degree a lower slope environment. Facies A + B + F constitute approximately 80 percent of the clastic rocks. Mutti and Ricci Lucchi (1972) suggest that large bodies of sandstone and conglomerate comprised predominantly of Facies A, B and F may result from in-filling of large submarine depressions incised into pelites of Facies G.

Tectonic setting

Clastic rocks of the Goddard area are here interpreted as submarine fan turbidity current deposits that have undergone imbricate thrust faulting in a subduction complex environment. Fold or thrust packets are typical of the deformational style of the Sitka Graywacke as mapped on the central west coast of Baranof Island. Thrust slices are common in the accretionary prisms of modern and ancient subduction zones (Karig and Sharman, 1975; Westbrook and Smith, 1983). The Sitka Graywacke on western Chichagof Island, which is also part of the Chugach terrane has been interpreted as part of a Cretaceous subduction complex by Decker (1980). Cowan (1982) suggested that the geologic history of this subduction complex includes a 1,000 km or more northwestward movement along a system of dextral transcurrent faults.

THE CRAWFISH INLET PLUTON

Introduction

Plutonic rocks of the Goddard Hot Springs vicinity constitute a 100 km2 northwestern portion of the Crawfish Inlet pluton (total exposure 540 km2). The Goddard area plutonic rocks are a heterogeneous mass of predominantly granodioritic and lesser tonalitic rocks with numerous inclusions in its western part. Two new K-Ar dates from a biotite-hornblende pair are 48.0 +- 1.4 and 48.3 +- 1.4 m.y. respectively indicating a middle Eocene age for the pluton (table 1). This agrees with five previous K-Ar ages on biotite separates which range from 43.1 and 48.1 m.y. (Loney and others, 1967). The Crawfish Inlet pluton is part of a Tertiary intrusive belt that crops out on the western side of the Alexander Archipeligo for over 350 km. Hudson and others (1979) included this pluton in their Sanak-Baranof belt, a 2000 km-long belt of discrete anatectic plutons that parallels the continental margin throughout the Gulf of Alaska region (figure 7). Igneous bodies of this belt intrude an upper Mesozoic and lower Tertiary accretionary prism of flyshoid rocks (Plafker and others, 1977).

Plutonic rock facies and modal mineralogy

In the Goddard area three gradational facies are recognized based on the following criteria: 1) composition from point count data and major oxide chemistry, 2) abundance of inclusions, 3) essential mineral grain size and morphology, and 4) accessory minerals. In a general east to west traverse (pluton core to margin) the three facies are: 1) the centrally located, homogeneous, xenolith-poor tonalite facies, 2) the more felsic and xenolith-rich granodiorite facies (which surrounds the tonalite facies) and, 3) the heterogeneous and xenolith-rich, locally peraluminous, locally primary white mica-

Table 1. Analytical data for K-Ar age determinations*.

Field No. (Lab No.) [Lat.& Long.]	Rock Type	Mineral Dated	K_2O(wt.%)	Sample Weight (g)	$^{40}Ar_{rad}$ (mol/g) x 10^{-11}	$^{40}Ar_{rad}/^{40}K \times 10^{-3}$	$^{40}Ar_{rad}/^{40}Ar_{total}$	Age ± 1σ (m.y.)
81RR170 (84119) [56°49'39"N 135°11'13"W]	Hb-Biotite Tonalite	Hornblende	0.340 0.330 $\bar{x}$ 0.335	1.5197	2.36	2.84	0.0985	48.3±1.4
81RR170 (84111) [56°49'39"N 135°11'13"W]	Hb-Biotite Tonalite	Biotite	9.120 9.120 $\bar{x}$ = 9.120	0.0804	63.9	2.83	0.772	48.0±1.4

Note: rad = radiogenic; σ = standard deviation; $\bar{x}$ = mean;

$\lambda_e + \lambda_e' = 0.581 \times 10^{-10}\ yr^{-1}$; $\lambda_\beta = 4.962 \times 10^{-10} yr^{-1}$;

$^{40}K/K_{total} = 1.167 \times 10^{-4}$ mol/mol.

*K-Ar determinations by J.D. Blum and D.L. Turner, Alaska Division of Geological and Geophysical Surveys, Geophysical Institute, University of Alaska, Fairbanks, Cooperative Geochronology Laboratory.

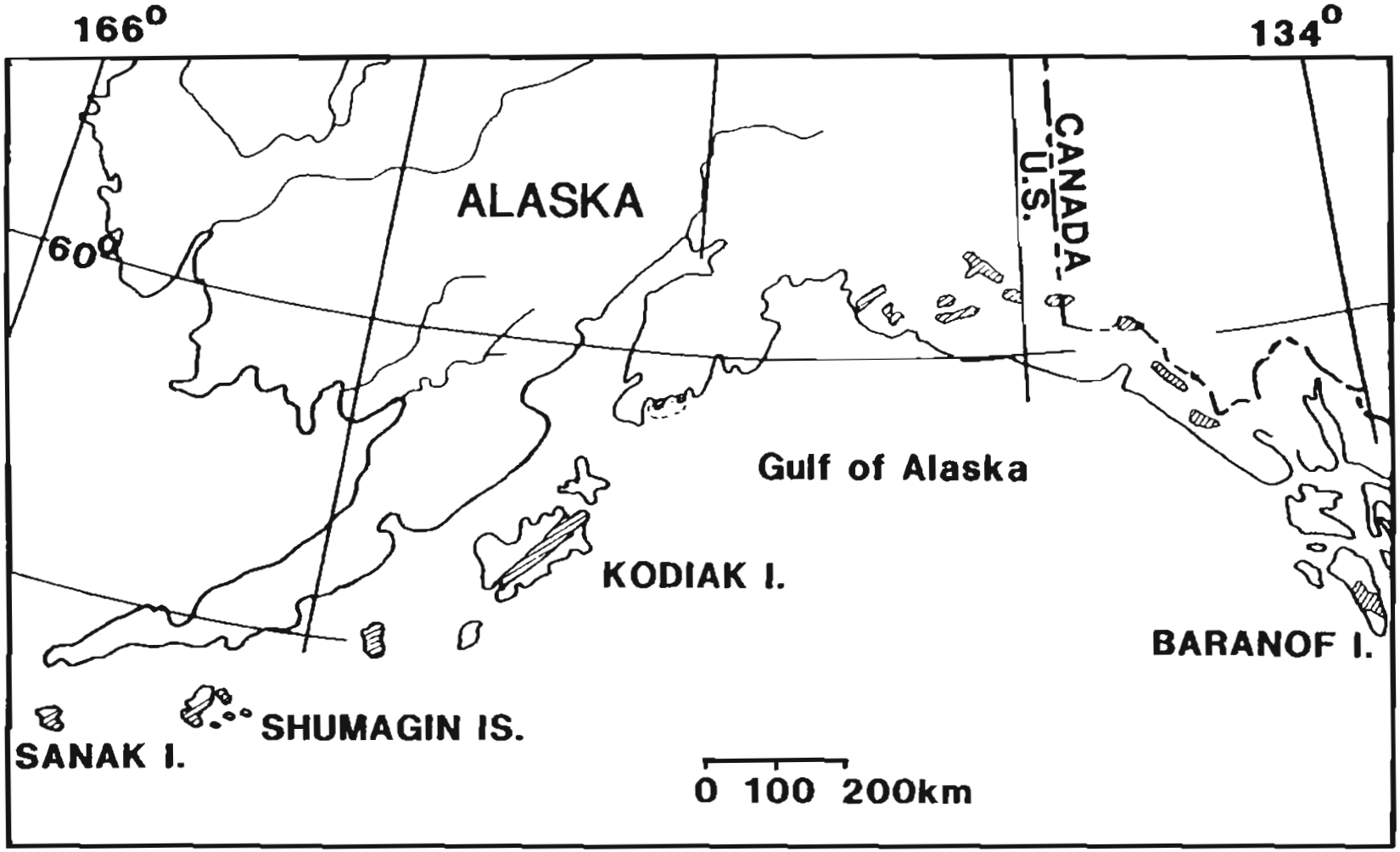

Figure 7. Location map of the Sanak-Baranof Tertiary anatectic intrusive belt (diagonal lines). Modified from Hudson and others, 1979.

bearing border facies (plate 1). The most common rock, all facies considered, is a medium- to coarse-grained hornblende-biotite granodiorite with a color index of 16 (point count data on 37 stained slabs). The compositions range from quartz monzonite to quartz diorite (figure 8). Hypidiomorphic-granular, and seriate textures are common, whereas coarse-grained porphyritic and allotriomorphic-granular textures are rare. The average modal composition is: 51 percent plagioclase, 24 percent quartz, 9 percent potassium feldspar, 12 percent biotite and 4 percent hornblende. Apatite, sphene and zircon occur as accessory minerals.

Contoured modal mineralogy values for hornblende, biotite, potassium feldspar, and hornblende as a percentage of total mafic minerals indicate that the plutonic rocks become more mafic to the east and southeast (figure 9). This orientation trends toward the geographic center of the Crawfish Inlet pluton. Modal mineralogy trends, therefore, suggest a reverse zoned pluton with more mafic and higher temperature minerals toward the pluton-center.

Goddard area plutonic rock facies

The tonalite facies

The tonalite facies underlies 38 km2 in the eastern and southeastern portions of the area mapped (figure 10; plate 1). This relatively homogeneous facies forms the center of the Crawfish Inlet pluton. The tonalite facies consists of medium- to coarse-grained, equigranular to seriate hornblende-biotite tonalite with an average color index of 19, and subordinant hornblende-biotite granodiorite. Igneous mineral foliation is typically absent but locally is weakly developed. Contact with the adjacent granodiorite facies is

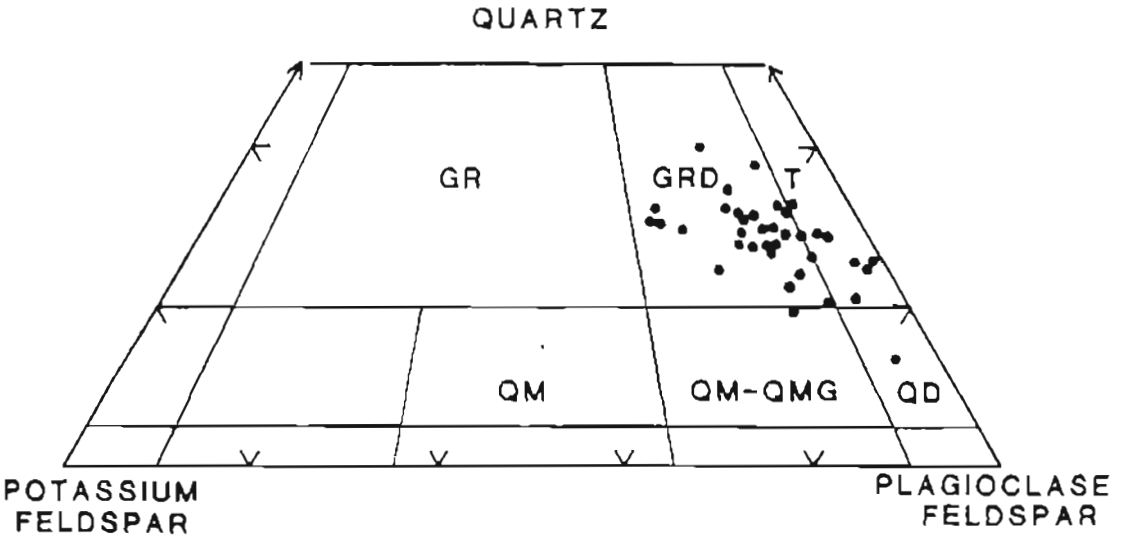

Figure 8. Modal potassium feldspar, quartz and plagioclase for 37 plutonic rocks from the northwestern portion of the Crawfish Inlet pluton plotted on the IUGS plutonic rock classification diagram (Streckeisen, 1973). Four hundred data points on stained slabs. GR=granodiorite, T=tonalite, QM=quartz monzonite, QM-QMG= quartz monzonite-quartz monzogabbro and QD=quartz.

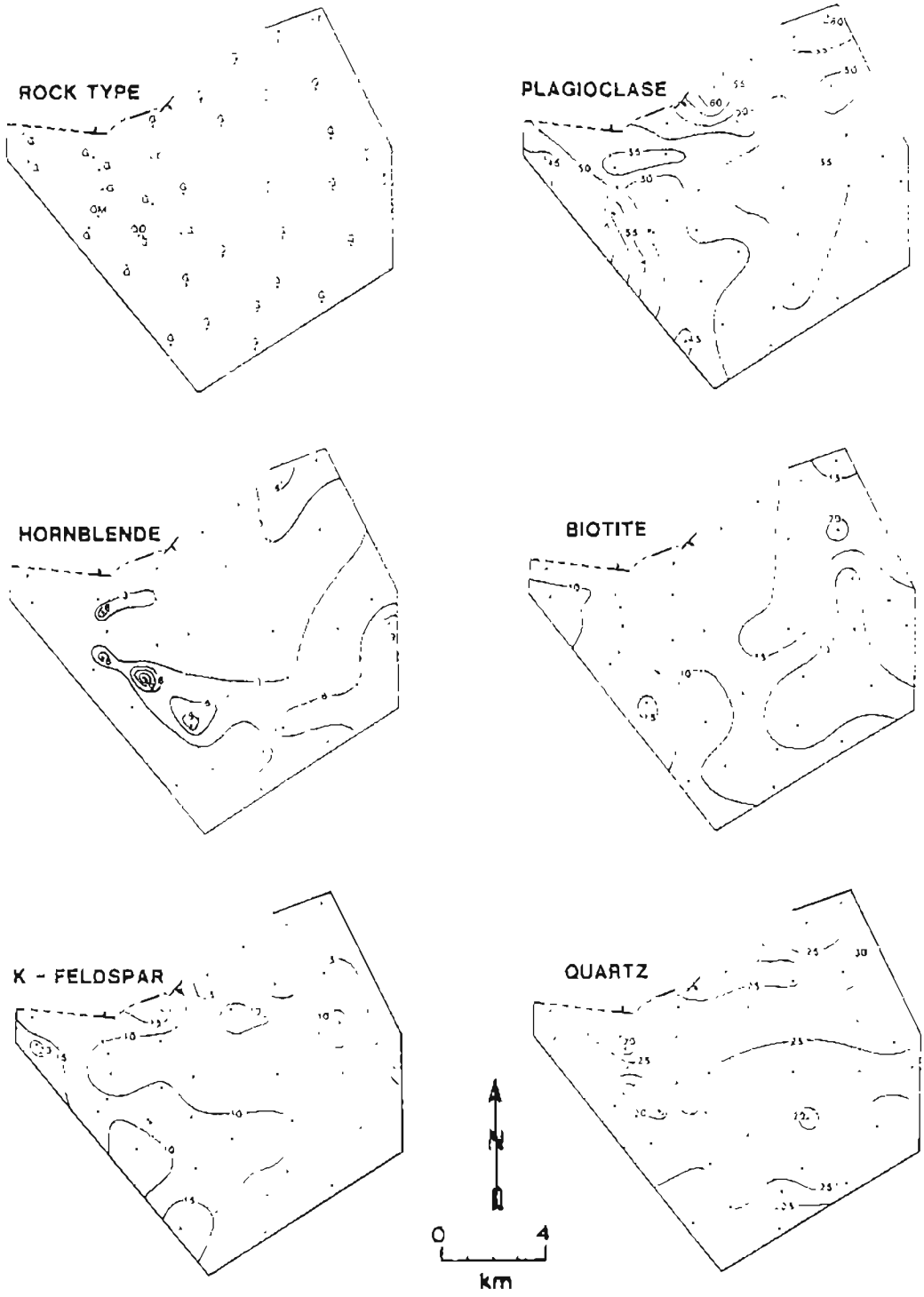

Figure 9. Distribution of minerals and rock type in a northwestern portion of the Crawfish Inlet pluton. Contours are in volume percent; T= tonalite, G= granodiorite, QD= quartz diorite, and QM= quartz monzonite.

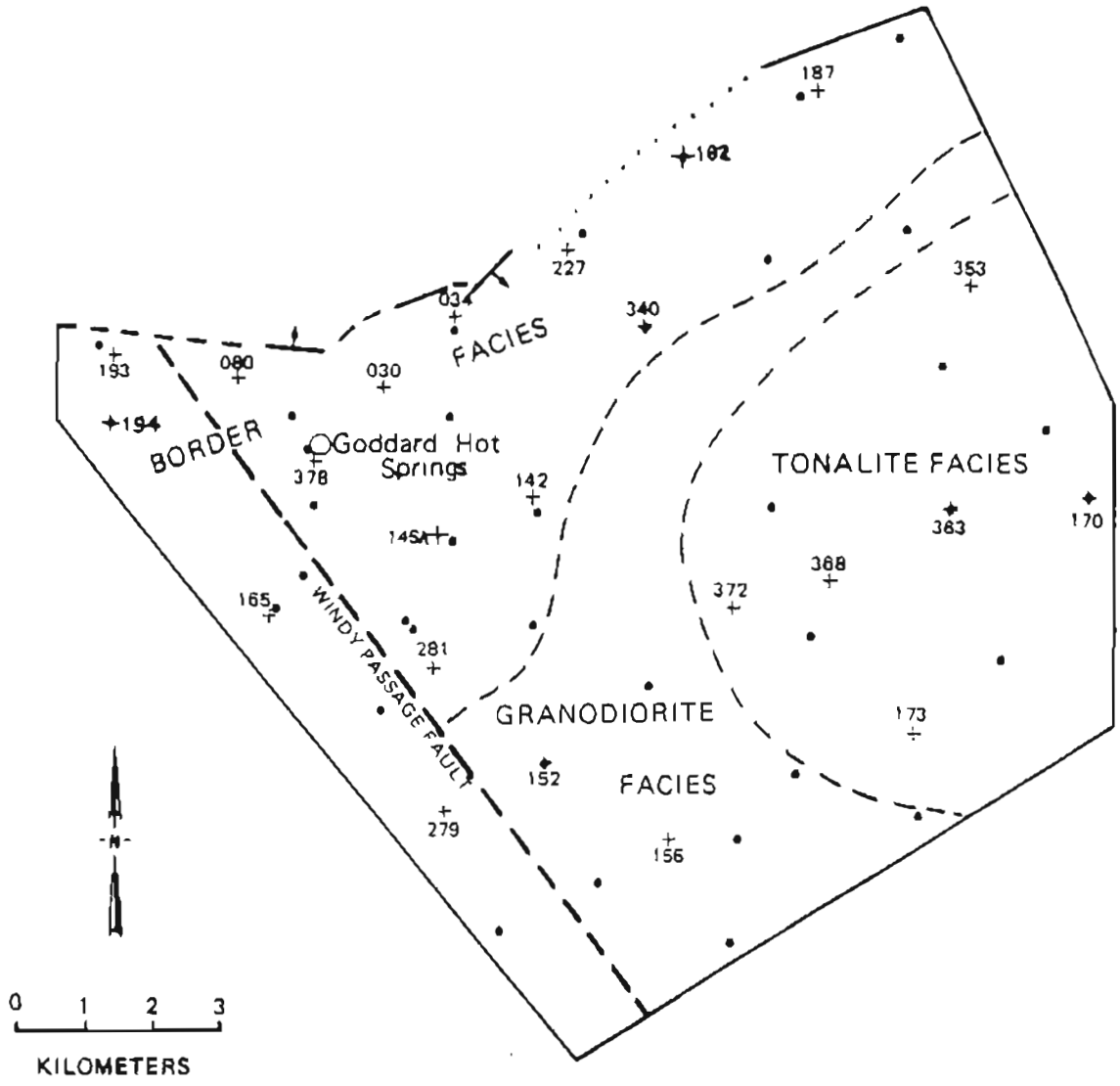

Figure10. Igneous rock facies of the northwestern portion of the Crawfish Inlet pluton. Dot is locality of point-counted, stained slab sample. Cross is locality of major oxide sample (Appendix 1).

gradational. Grains average 4 mm in diameter and the grain size range for these predominantly equigranular rocks is more limited than in other facies.

Rare xenoliths within the tonalite facies are foliated to massive, fine- to medium-grained, and contain biotite, plagioclase, and minor quartz. They form ovate-spheroid bodies less than 25 cm in diameter.

Mineralogy of the tonalite facies

In the tonalite facies hornblende is approximately 27 percent of the total mafic minerals; several percent higher than in the other facies. Hornblende occurs as 1 to 3 mm subhedral to euhedral crystals. Hornblende pleochroism typically is: X = yellowish green, Y = green, Z = greenish brown.

Biotite forms euhedral to subhedral six-sided 2.5 to 4 mm diameter crystals, and commonly forms books imparting a peppered appearance. Disseminated and fine-grained biotite is uncommon. Minor alteration to chlorite is common. Slight deformation of biotite crystals is common; plagioclase crystals are undeformed suggesting small scale syn-crystallization movement (Bateman and others, 1983).

Plagioclase feldspar typically occurs as 3 to 4 mm length normally zoned subhedral crystals, but may be as large as 10 mm. Generally fine-grained white mica alteration is minor. Plagioclase compositions average in the low andesine range (An33) with more calcic centers.

Quartz crystals form 1.5 to 6 mm across anhedral crystals with undulatory extinction. The last phase to crystallize in these rocks was potassium feldspar, which occurs as 1 to 2 mm interstitial anhedral crystals. Myrmekite growths in minor amounts are common.

The granodiorite facies

Rocks of the granodiorite facies underlie a 22 km2 area located between the centrally situated tonalite facies and the border facies. Contacts with the surrounding facies are gradational. The granodiorite facies consists of medium-gray, medium- and coarse-grained hypidiomorphic-granular to seriate hornblende-biotite granodiorite with minor hornblende-biotite tonalite. Average color index is 16. Average grain size is approximately 4 mm, and extremes of the 1 to 8 mm range are more common in this facies than the tonalite facies.

Xenoliths are more numerous in this facies than the tonalite facies. Typically they form less than 50 cm diameter bodies, and consist of fine- to medium-grained, granoblastic to foliated plagioclase, quartz, biotite, and locally potassium feldspar.

Mineralogy of the granodiorite facies

Hornblende occurs as 1 to 5 mm subhedral crystals with minor euhedral crystals. Hornblende pleochroism typically is: X= yellowish green, Y= green, Z= greenish brown to brown. Locally hornblende is altered to biotite and sphene.

Biotite typically forms subhedral crystals, locally occurs as euhedra with hexagonal outlines imparting a peppered appearance to the rock. Partial chloritization of biotite is common.

Plagioclase feldspar forms 2 to 8 mm subhedral, twinned and zoned crystals that average in the low andesine range (An31). Minor sericitic alteration is common.

Quartz and potassium feldspar occur as anhedral and interstitial phases respectively. Myrmekite is commonly present. Alteration products in the granodiorite facies include chlorite, white mica, epidote and sphene.

The border facies

The border facies underlies 38 km2 of the Goddard area plutonic rocks studied, and lies to the northwest, west and southwest of the granodiorite and tonalite facies. Contact with the adjacent granodiorite facies is gradational. The border facies rocks consist of medium-gray, medium-grained, with lesser coarse- and fine-grained, hornblende-biotite granodiorite and hornblende-biotite tonalite. Rocks of quartz diorite and quartz monzonite composition also occur. Textures include seriate, hypidiomorphic-granular and allotriomorphic-granular. Average grain size in this facies is about 3 mm and the range is the largest of all the facies: less than 1 mm to larger than 10 mm. The average color index is 15.

Xenoliths in the border facies are abundant, commonly large (over one hundred meters in diameter), and consist typically of plagioclase, quartz, biotite, and potassium feldspar, but locally contain white mica, garnet and cordierite.

Cordierite and garnet were each found at two localities and only in the border facies. The garnet occurs as 1.0 to 2.5 mm anhedral, fractured, disaggregated crystals suggesting relatively high instability. Here, alteration products of the garnet include chlorite,

epidote, white mica, and an opaque mineral. The garnets in the border facies may have formed during metamorphism of a pelitic country rock and then been entrained in the magma. Within xenoliths of the border facies, subhedral garnet appears stable suggesting that this phase is in equlibrium with the immediately surrounding restite. Garnet occurs as a xenocryst in an otherwise typical border facies igneous rock and shows evidence of disequlibrium with the surrounding primary igneous mineralogy. Disequilibrium is suggested by the physical disaggregation of the garnet. Presumably, chemical constituents are equilibrating with the surrounding quartz and plagioclase. Since garnet (assumed to be almandine) is a highly aluminous phase (approximately 21 percent Al2O3 - analysis from Deer and others, 1966) it appears to have been more throughly incorporated into the magma which had a tonalitic composition (Al2O3 = approximately 13 percent). The above garnet paragenesis in the border facies restite and igneous rocks suggests local melting of the country rocks. Schlieren and migmatite occur locally in the border facies and are restricted to the margin of the pluton.

Mineralogy of the border facies

Hornblende occurs as subhedral to anhedral crystals and is generally less than 4 percent of the rock with the following pleochroism: X=yellowish green, Y= green, Z= brown. Biotite is typically disseminated and rarely forms books. This habit is particularly evident in the southern part of Windy Passage where biotite in the adjacent granodiorite facies (across the strait to the east) forms well developed books. The border facies and the granodiorite facies may be juxtaposed by a fault in this strait.

Plagioclase forms subhedral, twinned and normally zoned crystals with a composition in the upper-most oligoclase range (An29).

Potassium feldspar typically occurs interstitially, however, it may form anhedral but distinct crystals. This mode of occurrence is not found in any other facies.

Primary white mica occurs in the border facies as 1 to 3 mm subhedral elongate crystals and is clearly not restricted to minerals it replaces. Garnet forms anhedral, equant 1 to 2.5 mm fractured and disaggregated crystals. The xenocrystic garnet is here interpreted to be from the paragneisses produced during metamorphism of a pelitic protolith. The garnet shows evidence of disequalibrium and is altered to white mica, epidote, chlorite and opaque minerals. The mineralogy of the border facies includes either white mica and, or garnet and, or cordierite or hornblende in addition to the ubiquitous feldspars, biotite and quartz.

Alteration products in this facies include chlorite, fine-grained white mica, epidote and sphene. Within 100 m of Goddard Hot Springs some specimens are partly- to almost wholly sericitized.

Major oxide chemistry

Major-oxide geochemical data suggest a reverse zoned pluton. A plot of six whole-rock, major-oxide values along a traverse from the xenolith-rich western margin to the relativly homogeneous and xenolith-free central core region clearly illustrates a more mafic composition toward the pluton center and a more felsic margin (figure 11). Samples to the west, within the border facies, are mostly granodiorite; samples to the east, (West Crawfish Inlet) within the tonalite facies are typically tonalites. The centrally located tonalitic rocks have higher values for Cao, Feo +Fe2O3, TiO2, MgO, and lower values for SiO2 and K2O. All major oxide data for the tonalite and granodiorite facies indicate metaluminous chemistry (mole proportions of CaO + Na2O +

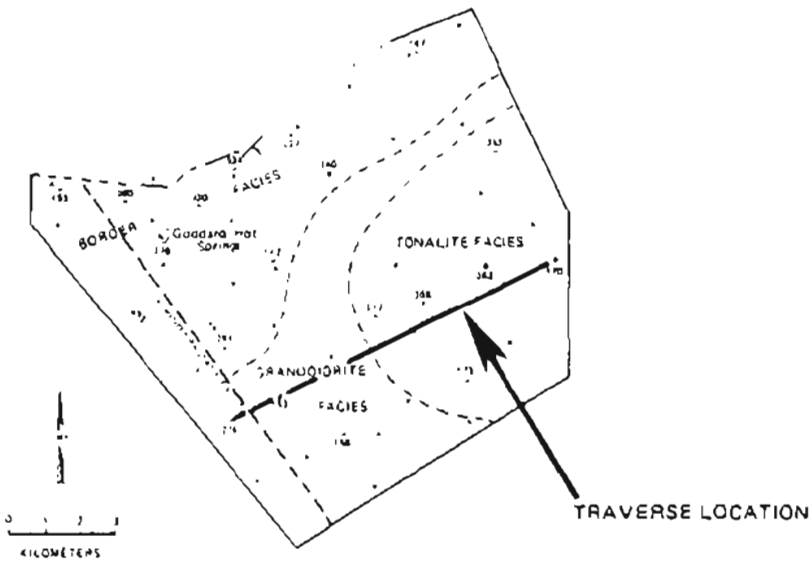

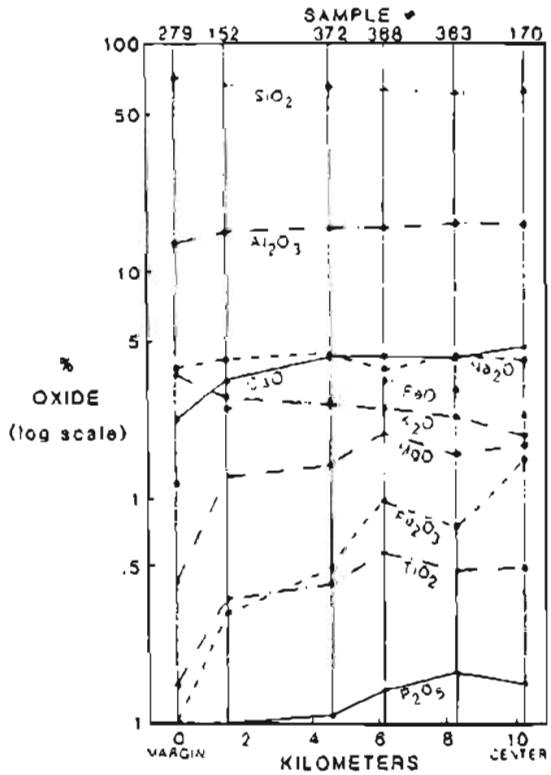

Figure 11. Plutonic whole-rock major oxides versus distance from edge toward the center of the Crawfish Inlet pluton for some Goddard area rocks.

K2O > Al2O3) and anorthite (An) is prominent in the norm (appendix 1). Biotite and hornblende occur as the dark Al-bearing phases.

Rock classification based on normative mineralogy using the classification of Barker (1979) yields rock classifications similiar to those obtained from modal mineralogy. However, the more silica-rich samples (>73 percent) plot close to, or in the granite field (figure 12), a more felsic designation than indicated on the modal mineralogy classification diagram (figure 9).

In the border facies seven of the thirteen major oxide samples are corundum normative (from 0.02 to 1.85 weight percent, appendix 1) and of these, four show peraluminous chemistry (figure 13). Within the Crawfish Inlet pluton only primary white mica occurs locally as an indicator of a peraluminous magma chemistry or protolith. White mica, where present, is relatively coarse grained (1.5 mm), subhedral and is not restricted to secondary mineral replacement. Goddard area peraluminous rock samples from the border facies contain no common mineralogic indicator of strongly peraluminous composition. However, in the border facies biotite is the dominant and locally the only mafic phase. Miller and Bradfish (1980) note that biotite is capable of accommodating into its structure up to 10 weight percent of excess aluminum. In weakly peraluminous rocks abundant biotite may, therefore, preclude the presence of a more strongly peraluminous phase. Two out of three border facies xenoliths yield peraluminous chemistry (figure 14), whereas only 3 out of 20 plutonic rock samples indicate peraluminous chemistry. The peraluminous xenoliths probably reflect partial melting of a pelitic protolith.

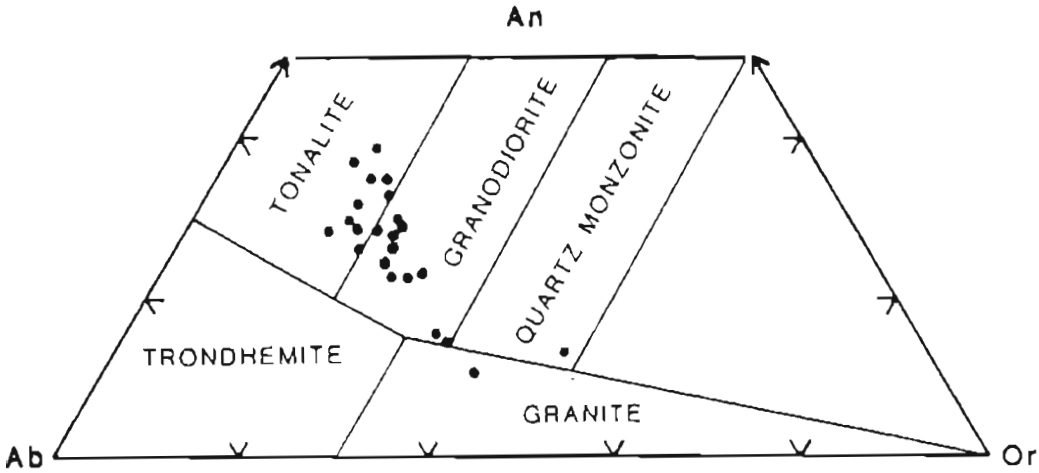

Figure12. Plot of normative albite, anorthite and orthoclase normalized to 100% for 23 plutonic rocks from the northwestern portion of the Crawfish Inlet pluton. Classification diagram from Barker (1979).

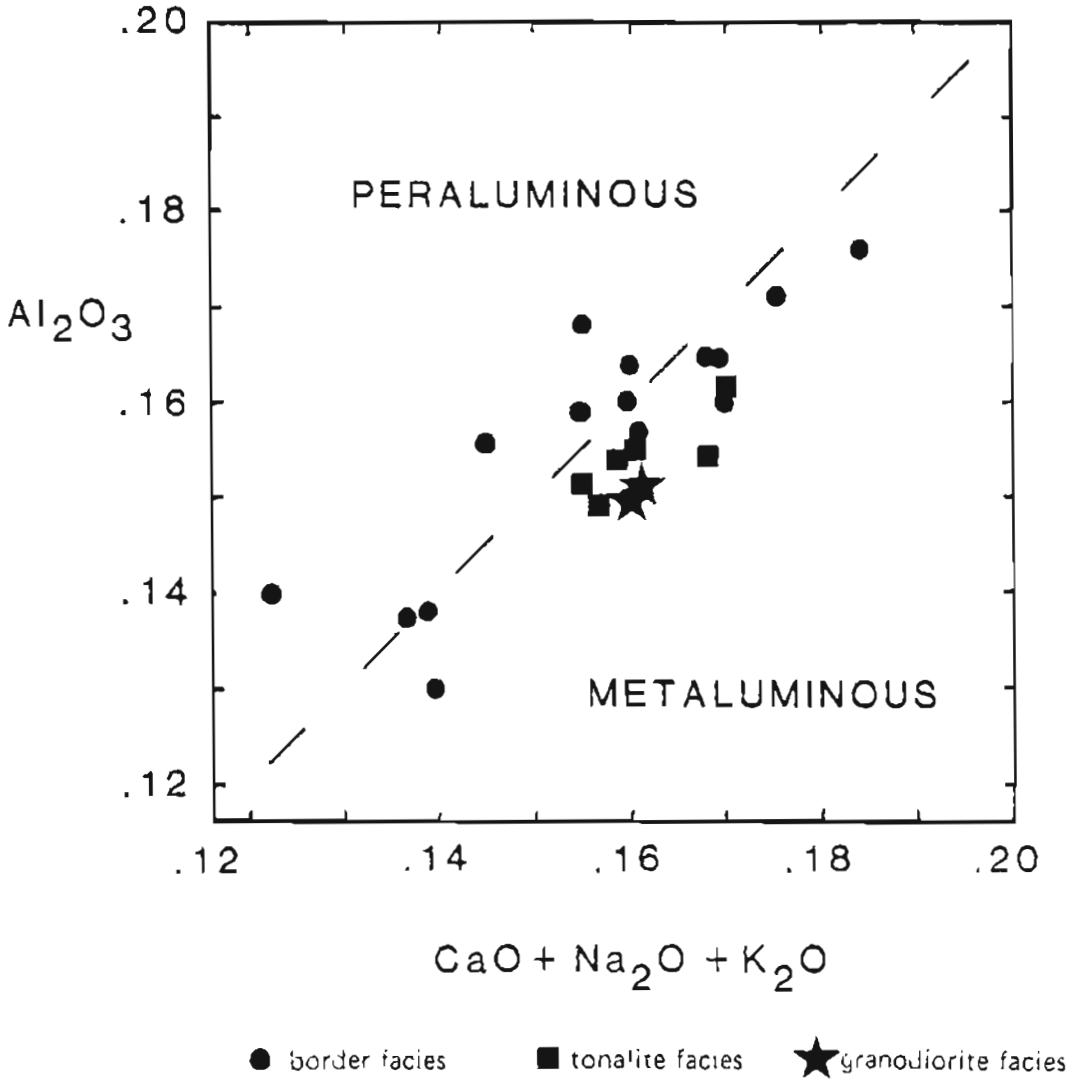

Figure 13. Al_2O_3 versus ($CaO+Na_2O+K_2O$) in molecular proportions for 23 samples from a northwestern portion of the Crawfish Inlet pluton.

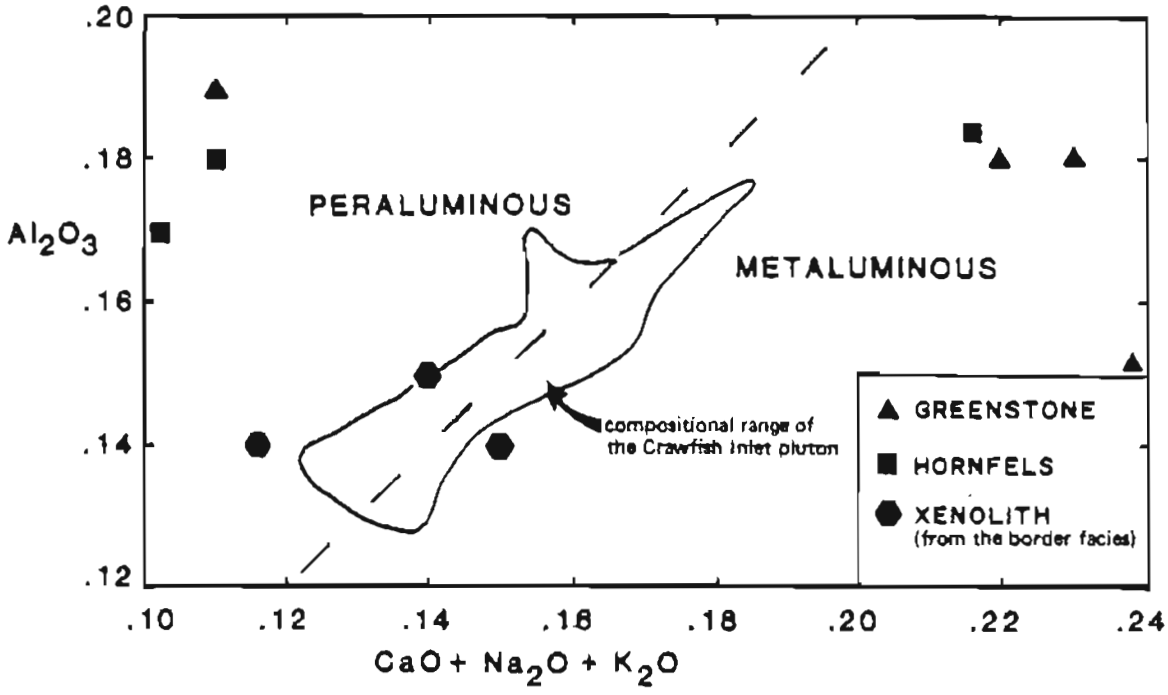

Figure 14. Al_2O_3 versus ($CaO+Na_2O+K_2O$) in molecular proportions for some greenstones, hornfels (both from the Sitka Graywacke) and xenoliths (from the Crawfish Inlet pluton) from the Goddard Hot Springs area.

Depth of crystallization

Results from experimental work by Tuttle and Bowen (1958) in the system $NaAlSi_3O_8$-$KAlSi_3O_8$-SiO_2-H_2O applied to an aplitic dike yield a pressure estimate (figure 15). This dike contains 9.8 percent normative An and due to this component a depth estimate will be a minimum (James and Hamiliton, 1969; Swanson, 1978). The melting relations shown in figure 15 yield a pressure estimate of just less than 2 kb for the Goddard aplite dike, indicating a moderate to shallow crystallization depth for these rocks.

Pluton consanguinity

I interpret the three facies of the Crawfish Inlet pluton to be comagmatic on the basis of field, petrographic and major-oxide geochemical data (23 samples). A plot of the differentiation index (normative Q+Or+Ab+Ne+Ks+Lc) vs the normative plagioclase composition (normative An x 100/An + Ab + 1.67Ne) yields a tight linear trend (figure 16) supporting consanguinity. Plotted on an igneous AFM diagram these data delineate a well defined calc-alkaline trend, plotting approximately normal to the MgO-FeO* side (figure 17). The linear trend on the AFM diagram also supports comagmatism.

Rubiduim and strontium isotopes

Six Crawfish Inlet pluton samples and two Sitka Graywacke samples analyzed for rubidium, strontium, and strontium isotopic composition (table 2) place some restrictions on magma genesis. Rubidium-strontium ratios cover a wide range (0.704 -71.2), however five of the plutonic rock analyses yield similiar values and lie close to the 87Sr/86Sr intercept. The sixth sample, an aplite dike, yields a 87Rb/86Sr value of 71.2,

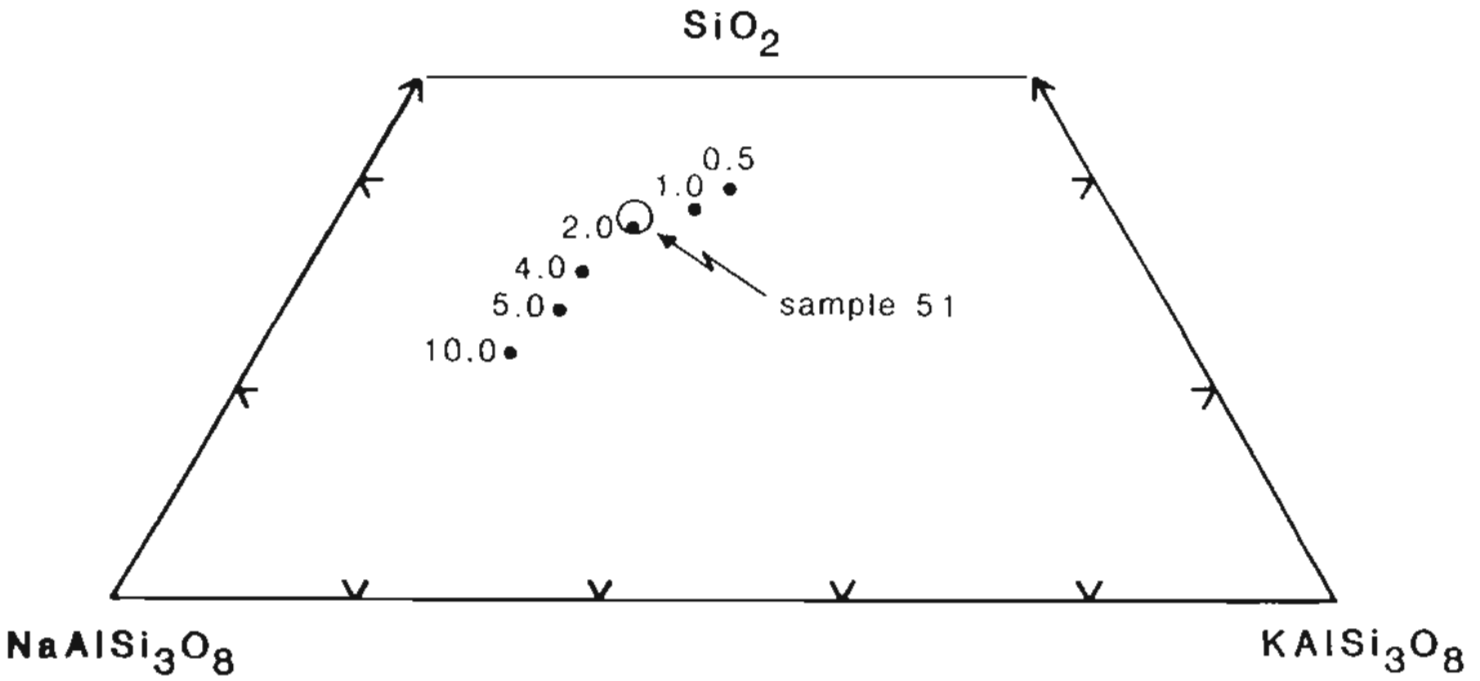

Figure 15. Plot of normative albite, orthoclase and quartz (normalized to 100%) for an aplitic dike of Crawfish Inlet pluton. Shift of isobaric minima in the system $NaAlSi_3O_8$-$KAlSi_3O_8$-SiO_2-H_2O with increasing pressure is also shown (Tuttle and Bowen, 1958; Luth and others, 1964). Numbers are kilobar values.

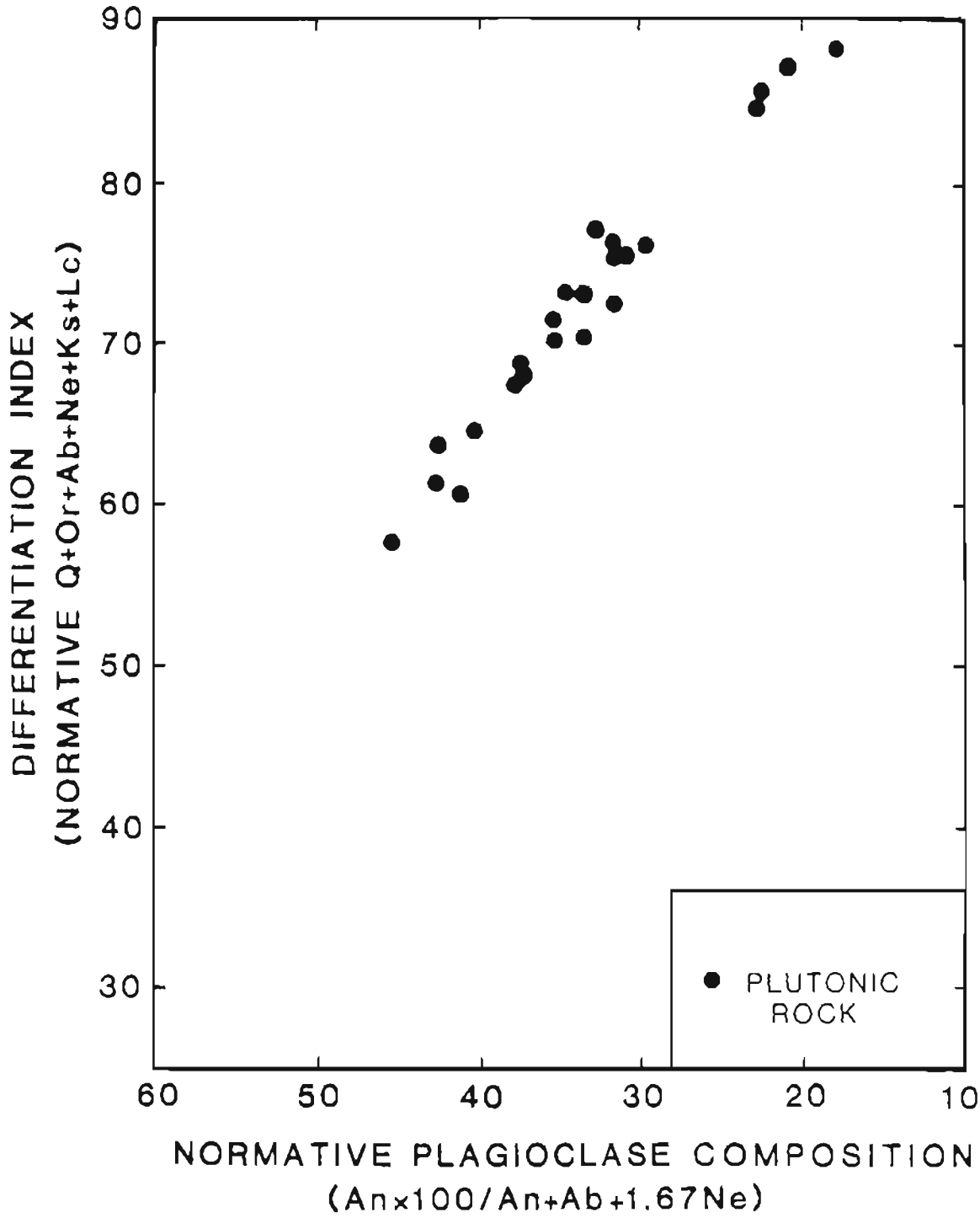

Figure 16. Plot of differentiation index versus normative plagioclase composition for some igneous rocks of the Goddard area.

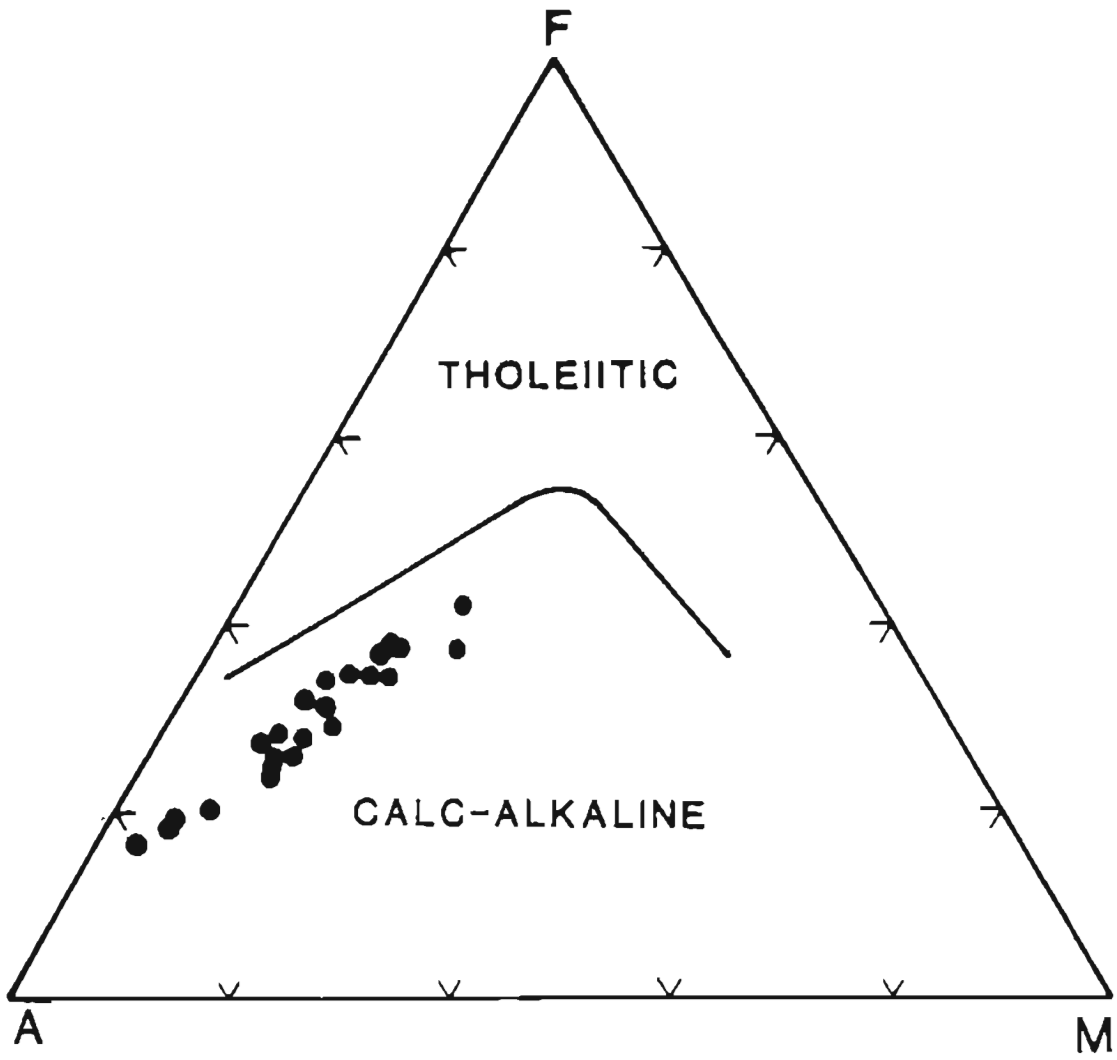

Figure 17. AFM variation diagram for 23 samples from the northwestern portion of the Crawfish Inlet pluton. A= (Na_2O+K_2O), F= ($FeO+0.9\ Fe_2O_3$); M= MgO. Tholeiitic/calc-alkaline line from Carmichael and others (1974).

Table 2. Rubidium-strontium data from the Goddard area.

Sample no.	87Sr/86Sr	Sr(ppm)	Rb(ppm)	86Sr	87Rb	87Rb/86Sr	Rock type
81RR168	0.70532	204	74.2	20.1	20.7	1.03	Tonalite
81RR230	0.70653	177	120.0	17.5	33.4	1.91	Granodiorite
81RR390	0.70524	228	69	27.4	19.3	0.704	Tonalite
81RR141	0.70606	262	129	25.8	35.9	1.39	Granodiorite
81RR145	0.70533	308	205	30.3	57.2	1.88	Quartz diorite
81RR172	0.74163	7.8	197	0.77	54.8	71.2	Aplite dike
81RR024	0.70661	313	99	31.0	28.0	0.9	Siltstone
81RR075	0.70641	508	67	50.0	18.7	0.37	Sandstone

Analyses by Dr. Terry Davis, Department of Geology, California State University, Los Angeles, California.

thereby controlling the slope of the isochron (normally taken as the crystallization age). Sample number 81RR145 data are unreliable since numerous partially assimilated country rock xenoliths occur within 2 m, suggesting contamination. An isochron based on the four reliable plutonic samples and the aplite yield an age of 12.5 m.y. with an initial ratio of 0.70514. K-Ar data tightly constrain the age of this pluton: 48.0 and 48.3 m.y. on a hornblende-biotite pair (this study) and 43.1 to 48.1 m.y. on five biotite separates (Loney and others, 1967). On the basis of this age control and geologic field relationships the 12.5 m.y. isochron is considered invalid. An isochron through the four uncontaminated plutonic rocks (figure 18) yields a 69.3 m.y. age and an initial ratio of 0.70432. The 69.3 m.y. isochron-age is suspect, in part, because the pluton intrudes Upper Cretaceous strata.

Initial $^{87}Sr/^{86}Sr$ ratios, calculated using the 48.0 m.y. age, range from 0.70464 to 0.70527. These ratios lie within the range of Phanerozoic orogenic batholiths, typically 0.704 - 0.709 (Cox and others, 1979). Crawfish Inlet pluton initials do not indicate interaction with highly isotopic crust. The range is not high enough to exclude the possibility of partial melting of an accretionary wedge composed of Mesozoic volcanic and plutonic-rich sediments such as the Sitka Graywacke. However, an anatectic petrogenesis, on the basis of various geologic evidence cited above, is not required. The preferred petrogenetic model yields intermediate initial ratios by contamination of a mantle-derived magma by assimilation of older crustal material.

Conclusions

Petrologic and chemical data suggest that during emplacement of the Crawfish Inlet pluton the central core area remained at a relatively high temperature. This resulted in a homogeneous, xenolith-free, hornblende-rich, potassium feldspar-poor core, a xenolith-

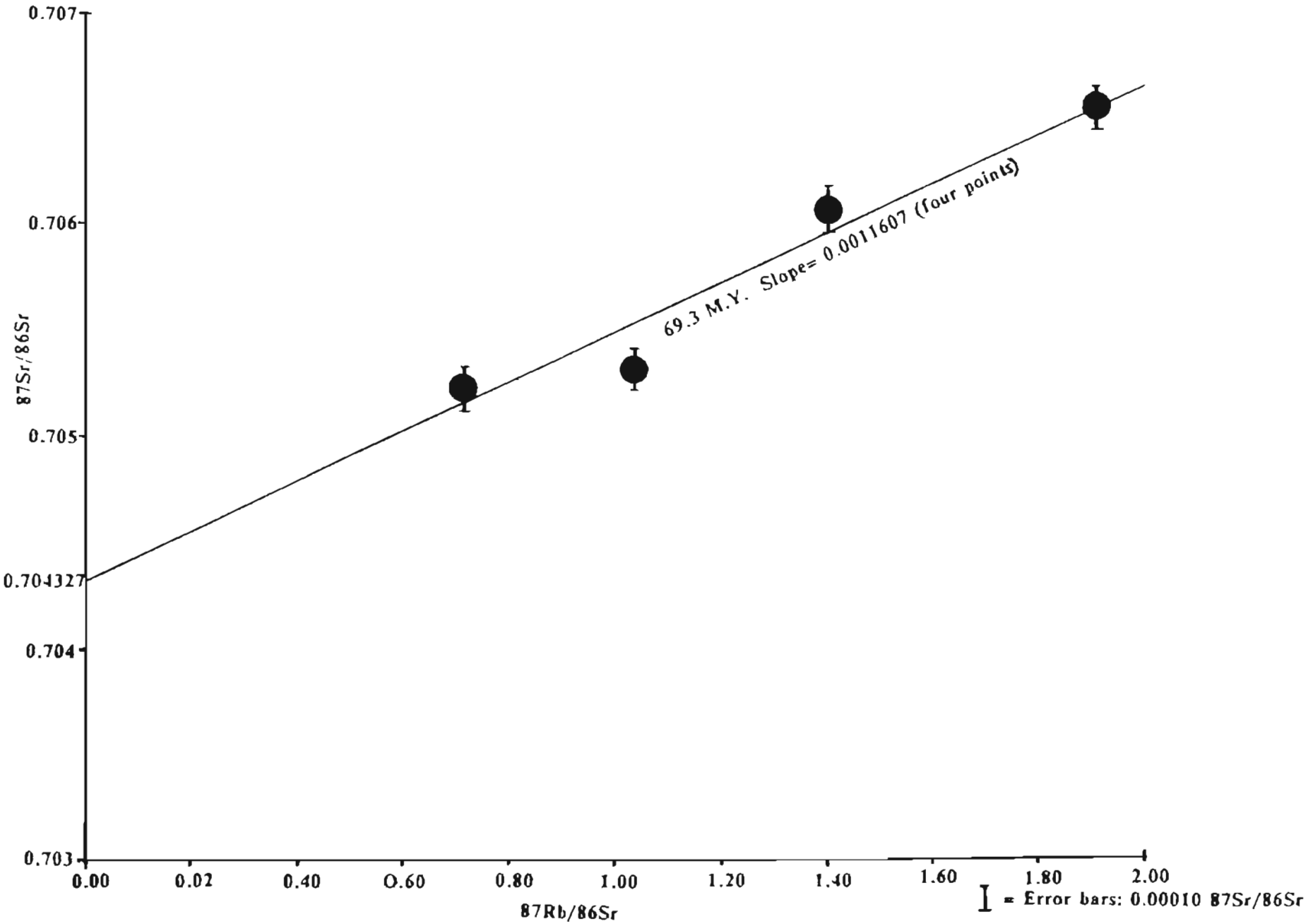

Figure 18. Values of 87Sr/86Sr and 87Rb/86Sr for the Crawfish Inlet pluton plotted on an isochron diagram.

rich, lower temperature border zone; ultimately yielding a reverse-zoned pluton. Mineralogy of the country rocks intruded by the pluton indicates hornblende hornfels facies metamorphism. The P-T environment of the country rocks must have been lower than that of the magma, indicating a migration of the magma from depth.

Hudson and others (1979) have suggested an anatectic origin for the Sanak-Baranof belt of plutons. Data from the Goddard area suggest an overall non-anatectic paragenesis, though minor partial melting along the margin of the pluton occurs locally. Several lines of evidence have been considered: 1) Xenocrystic phases. Phases that appear to be xenocrysts in the border facies include biotite, cordierite, garnet, and white mica. 2) Migmatization. Migmatite is common in border facies rocks. 3) Geologic setting. Differential partial melting of country rock bulk compositions are capable of yielding observed range of igneous and xenolith mineralogies (consistant with experimental data of Winkler (1979) in the system Qz-Ab-An-Or-H2O). 4) Modal mineralogy zonation. More mafic mineralogy and higher temperature trends occur toward the center of the pluton. 5) Hornblende is a normally occurring phase. 6) Whole-rock, major-oxide geochemistry. Consistantly more mafic affinities are toward the center of the pluton. Seven of the 23 plutonic rock samples indicate normative corundum and four samples indicate peraluminous chemistry. 7) Pluton heterogeneity. Modal mineralogy, major oxide values and xenolith occurrences are generally variable. 8) Xenolith occurrences. Xenoliths are numerous, and may be extensive.

A metaluminous to peraluminous compositional trend occurs from the tonalite and granodiorite facies to the border facies. One explanation for the trend is the assimilation of peraluminous country rock into a metaluminous magma. Alternatively, fractional crystallization of hornblende (normally metaluminous) and timing and quantity of biotite

crystallization also can control whether late-stage magmatic evolution yields a peraluminous melt (Zen and Hammerstrom, 1983).

The compositional range of the Crawfish Inlet pluton overlaps the range of Sanak-Baranof belt of anatectic plutons (figure 19) but typically contains more plagioclase, less quartz and one to six percent more hornblende. Also, the overall modal mineralogy, heterogeneity and the seriate texture suggest that the Crawfish Inlet pluton is not part of the Sanak-Baranof belt of Hudson and others (1979).

Rb and Sr data do not form a reliable isochron, and may indicate local contamination by heterogeneous country rock. An isotopic-rich crustal source is not indicated but the magma's origin can not be exclusively defined. The preferred petrogenetic model is crustal contamination of a mantle-derived magma.

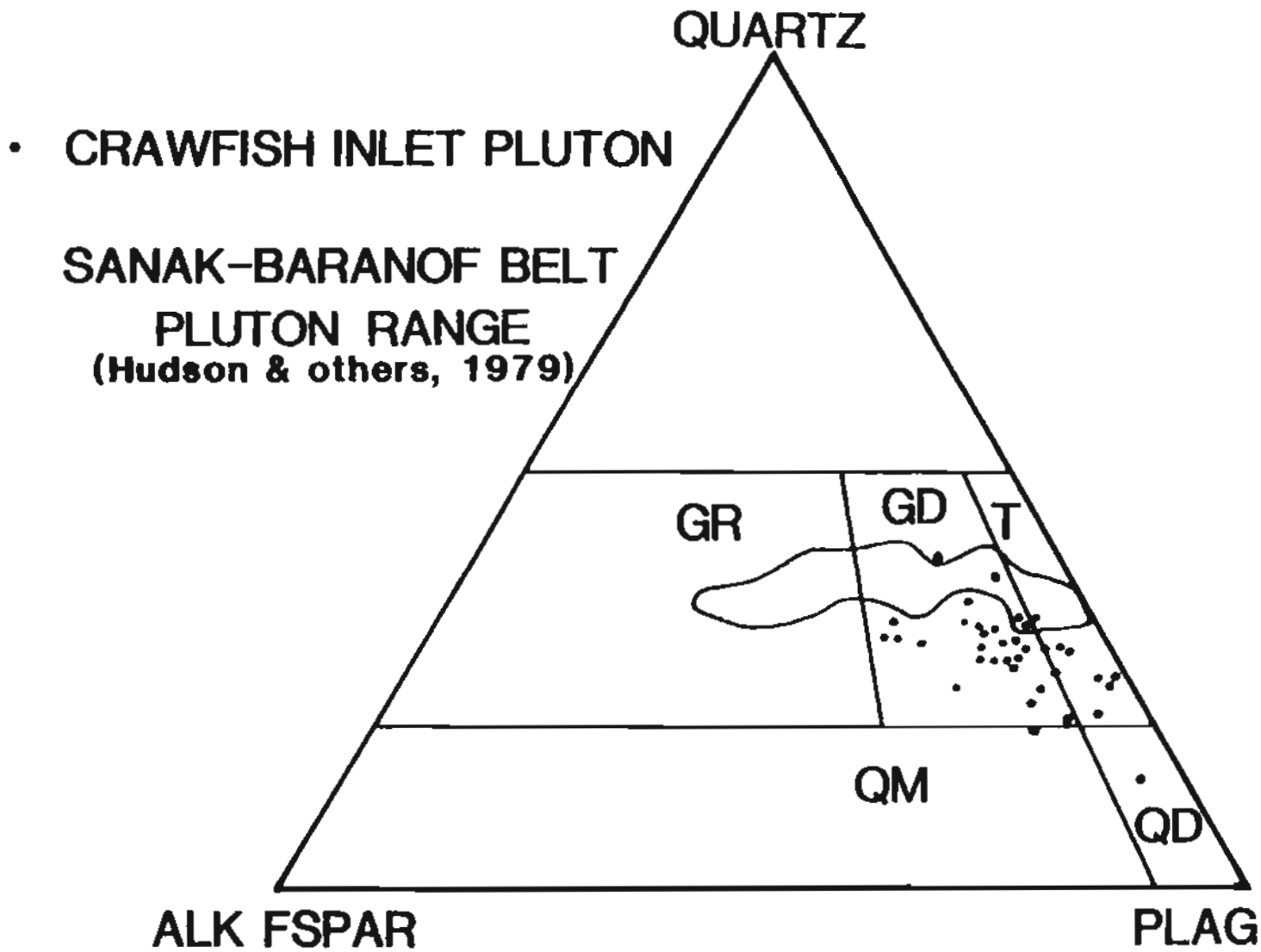

Figure 19. Compositional range of Sanak-Baranof plutons (Hudson and others, 1979) and compositions of the Crawfish Inlet pluton (37 stained slabs; 400 points each). GR= granite, GD= granodiorite, T= tonalite, QM= quartz monzonite, QD= quartz diorite.

CONTACT METAMORPHIC ROCKS

Introduction

The Crawfish Inlet pluton produced a contact metamorphic aureole that is from 3 to 3.5 km wide but locally extends up to 4 km into the Sitka Graywacke. The boundary of the outer aureole was placed at the first field-observed occurrence of metamorphic biotite.

Biotite zone - outer aureole

Recrystallization in this zone is moderate; sedimentary structures are typically well preserved. Laterally continuous and finely laminated planar turbidite features are well preserved. The metamorphic mineral assemblage in the outer aureole consists principally of biotite, plagioclase and quartz.

Hornblende hornfels facies - inner aureole

Hornblende-hornfels facies metamorphism is developed in a contact aureole around the Crawfish Inlet pluton and is locally up to 2 km wide. Locally rocks in this facies are foliated indicating that dynamic in addition to thermal metamorphism was important here. A mafic volcanic sequence in Kanga Bay yields the assemblage of hornblende (55 percent), plagioclase (40 percent) opaque minerals (5 percent) and sphene (minor). Graywacke and hemipelagic shale sequences less than 1 km from the pluton contact typically contain quartz, plagioclase, biotite, white mica, cordierite, and locally garnet. Cordierite typically occurs as incipient porphyroblasts. Aluminosilicate (Al2SiO5) polymorphs were not found and their absence is probably a function of the protolith bulk composition (figure ~~19~~ 20). Plotted on a metamorphic AFM diagram the bulk

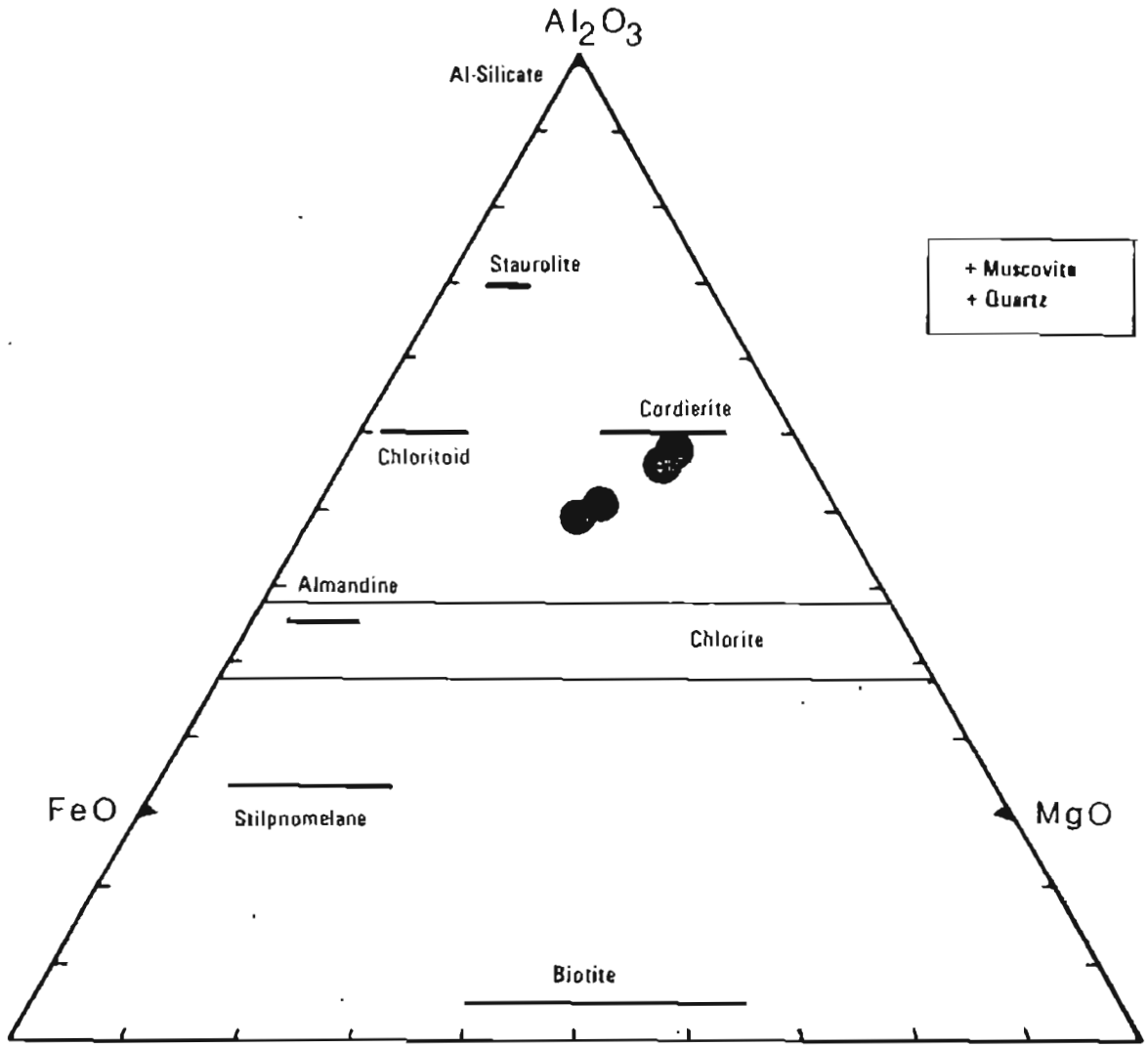

Figure 20 Mineral compositions plotted on the AFM projection plane. The common range of compositions is indicated by a line. Circles represent the bulk composition of Sitka Graywacke samples. From Winkler, 1979.

compositions of fine grained clastic rocks from the Sitka Graywacke indicate an only moderately aluminum-rich value for the system. The protolith composition lies in a triangle with the apicies cordierite, almandine and biotite.

Pressure-temperature restrictions

The mineral assemblages produced by contact metamorphism yield some restrictions on pressure-temperature estimates of metamorphism. Lack of good pressure-temperature control is due to the stability curves on a petrogenetic grid of the metamorphic mineralogy developed in the metagraywacke and metavolcanic rocks: biotite, plagioclase, quartz, hornblende, muscovite, cordierite, and garnet. Pressure-temperature values consistant with the paragenesis range from 1 kb to more than 5 kb and from 525°to 650°C. The approximately 2 kb value determined from an aplite dike of the Crawfish Inlet pluton is the preferred pressure value and is within the range indicated by the metamorphic mineral assemblage.

HYPABYSSAL DIKES

Steeply dipping dikes are common in the Goddard area, and range in thickness from <10 cm to 15 m (figure 21). Dike lithologies are: (1) felsic, (2) hornblende diabase, and (3) alkali-olivine diabase. These dikes cross-cut the Upper Cretaceous Sitka Graywacke and the middle Eocene Crawfish Inlet pluton. Several dike outcrops clearly show evidence of glacial erosion. The cross-cutting relationships and the glaciation indicate a post-48 m.y. and pre-Pleistocene age of emplacement.

Felsic dikes

Dikes range in composition from rhyodacite to dacite and are porphyritic with medium-grained subhedral andesine phenocrysts in a fine-grained matrix of randomly oriented plagioclase laths and quartz. Alteration products include chlorite and calcite. Locally, hornblende occurs and is altered, in part, to chlorite, sphene, calcite and opaque minerals.

Hornblende diabase dikes

The hornblende diabase dikes are fine-to medium-grained and consist of approximately 50 percent plagioclase and quartz, 40 percent hornblende, 5 percent vesicles filled with zeolite or microcrystalline chlorite, 5 percent opaques, and locally minor augite. The plagioclase (labradorite) occurs as relatively fresh, randomly oriented, subhedral laths; locally altered to epidote. Hornblende occurs as reddish-brown subhedral crystals.

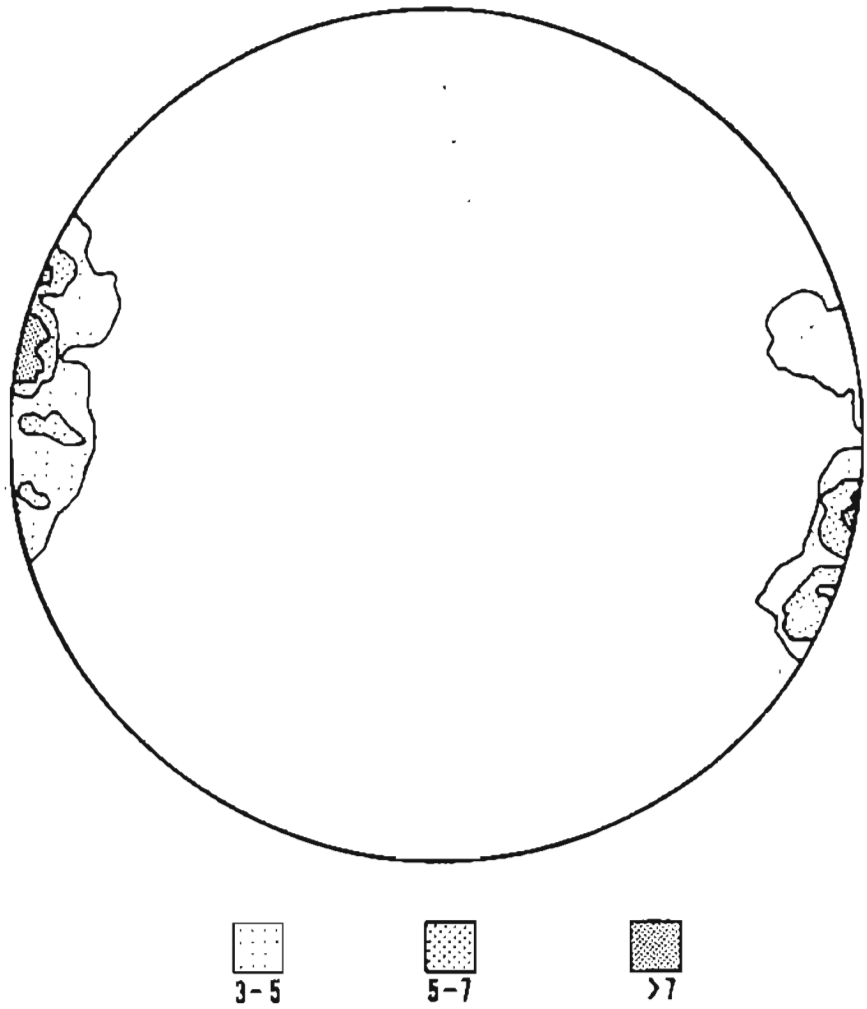

Figure 21. Lower hemisphere, equal area projection of attitudes of 35 hypabyssal dikes from the Goddard area. Contours in frequency of occurrence.

Alkali-olivine diabase dikes

The alkali-olivine diabase dikes are veryfine- to fine-grained, black, amygdaloidal, dark brown-weathering rocks. The dikes have a subophitic texture and are composed of granular, anhedral to prismatic titanaugite (based on pleochroism), randomly oriented laths of labradorite, and equant, anhedral olivine. The olivine is partially altered to a reddish-brown material, probably iddingsite. Locally, sub-parallel plagioclase laths yield a well developed trachytic texture.

Dike chemistry

Plotted on an AFM variation diagram mafic dike compositions lie on, or very close to, the calc-alkaline/tholeiitic line (figure 22) and it is not entirely clear which trend is represented. However, the mafic dike values plotted on a SiO2 versus FeO(total)/MgO diagram of Miyashiro (1974) clearly indicate tholeiitic affinities (figure 5). Kosco (1981) recognizes tholeiitic olivine basalt lavas on Mt. Edgecumbe, a Holocene stratovolcano located 30 km northwest of Goddard Hot Springs. The Goddard olivine-bearing dikes are probably related to the Edgecumbe Volcanics.

Loney and others (1975) suggested a probable comagmatic origin for the alkali-olivine dikes and the Edgecumbe Volcanics. Mineralogy, tholeiitic trend, age of emplacement, and outcrop location of the alkali-olivine dikes are consistant with a comagmatic origin with the Edgecumbe Volcanics. The comagmatic interpretation of Loney and others (1975) was based, in part, on the Mount Edgecumbe caldera lying on an extrapolation of the Windy Passage fault which they suggested was an access route for the basaltic magma.

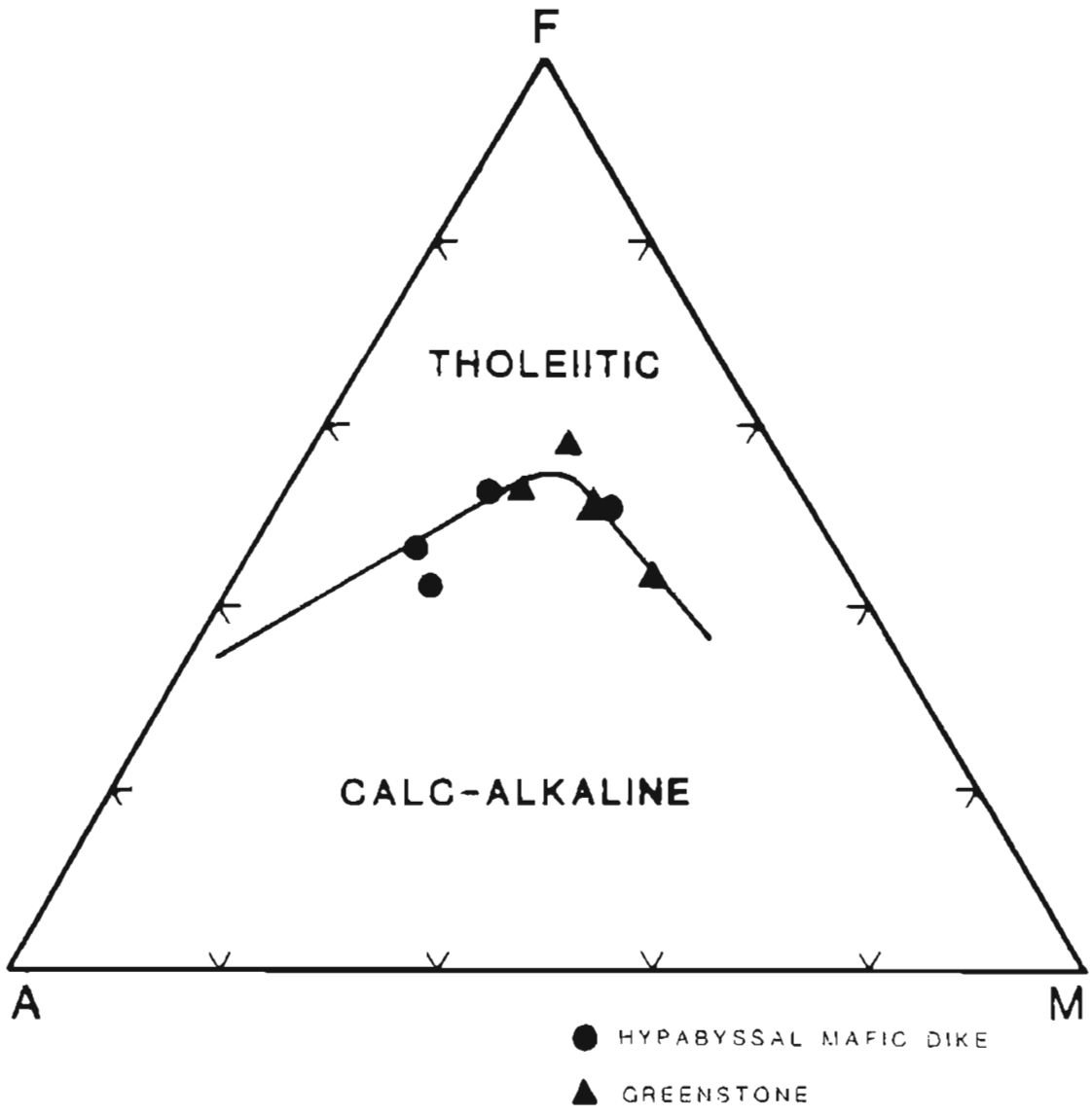

Figure 22. AFM variation diagram for some greenstones and mafic dikes from the Goddard area. A= (Na_2O+K_2O), F= ($FeO+0.9Fe_2O_3$); M=MgO. Tholeiitic/calc-alkaline line from Carmichael and others (1974).

GODDARD HOT SPRINGS

Introduction

Goddard Hot Springs consist of four surface hot spring seeps located 24 km south of Sitka, Alaska. Waring (1917) named them: Main, Magnesia, Sulfur and Old Russian Hot Springs. All the springs lie within 70 m of each other, issue at an elevation of between 15 m and 24 m above mean high tide, and lie 120 m to 140 m inland. The individual flow rates range from 38 to less than 1 liter/minute. The temperature of the hot water at the surface varies from 65.6°C in the main spring to 50.1°C in the sulfur spring.

Fluid geochemistry

The fluid geochemistry of the hot springs indicates that the four are similar in SiO2, K, Na and pH. Only the alkalinity (based on HCO-3) of the magnesia spring is markedly different from the other three (the high HCO3 value is suspected by the water chemist of being inaccurate). The values obtained from the present chemical species analysis (table 3 and table 4) are in close agreement with those of Bliss (1983) and Waring (1917), (table 5). The chloride species constitutes more than 50 percent, and sodium more than 26 percent of the total dissolved solids. Thus, the saline-rich hot water is essentially a weak brine. The level and ratio of the sodium and sulphate species and other constituents suggest that the hot waters are related in part to the nearby sea water.

Table 3. Geochemical data on Goddard Hot Springs. Units are mg/l unless otherwise noted. Water chemistry by Mary Moorman, Alaska Division of Geological and Geophysical Surveys.

	Magnesia Spring	Main Spring	Sulfur Spring	Old Russian Spring
SiO_2	107	107	107	107
Fe	0.18	0.19	0.20	0.22
Ca	351	353	351	352
Mg	1.5	1.6	1.7	1.4
Na	1286	1344	1333	1315
K	63.7	66.2	64.3	63.0
Li	1.62	1.64	1.64	1.61
HCO_3	237	59	58	69
SO_4	90.4	90.4	88.0	88.4
Cl	2720	2750	2735	2710
F	1.68	1.68	1.66	1.64
B	1.0	1.0	1.0	1.0
Sr	3.4	3.5	3.4	3.4
ph, field	7.12	7.12	7.26	6.90
Hardness (mg/l $CaCO_3$)	887	892	888	890
Sp conductance (μmhos/cm at 25°C)	8000	8500	8500	8000
T(°C)	65.3	65.6	50.1	51.9
Date sampled	5-30-81	5-30-81	5-31-81	5-31-81

Table 4. Geochemical data on some Goddard area cold water streams. Units are mg/l. Water chemistry by Mary Moorman, Alaska Division of Geological and Geophysical Surveys.

	Cold Stream 2 (raw, unfiltered)	Cold Stream 3 (raw, unfiltered)	Cold Stream 3 (filtered and acidified)
SiO_2	6	2.5	Not done
Fe	0.21	0.11	0.45
Ca	9.5	8.2	1.2
Mg	1.4	0.9	0.5
Na	48	40	6.7
K	1.08	1.46	0.11
Li	0.04	0.04	0.0
HCO_3	Not done	Not done	Not done
SO_4	1.6	1.6	0.0
Cl	87	71.0	69.2
F	1	1	1
B	0	0	0
Sr	0.0	0.0	0.0
Dissolved solids	154.6	125.7	77.7
Hardness (mg/l $CaCO_3$)	29.5	24.2	5.06
Sp conductance (µmhos/cm at 25°C)	350	250	70
Temperature (°C)	9.7	9.4	11.6
Flow rate (liters per minute, estimate)	10-20	10-20	Not done
Date sampled	5-31-81	5-31-81	5-31-81

Table 5. Geochemical and isotopic data, Goddard Hot Springs and area cold stream, from previous workers. Units are mg/l unless otherwise noted.

	U.S. Geological Survey (1983)		Waring (1917)
	Main Spring	Cold Water Spring	Main Spring
SiO_2	120	--	96
Ca	380	--	378
Mg	1.9	--	7.2
Na	1500	--	1440
K	61	--	60
HCO_3	78.7	--	29
Cl	2780	--	2745
F	1.4	--	--
CO_3	0.3	--	0.0
Total dissolved solids	5041	--	4877
pH	7.37	--	--
Temperature	67°C	--	149°F(65°C)
Deuterium	-82.8	-63.3	--
Oxygen-18 (permil)	-11.10	- 8.67	--

Geothermometers

A variety of chemical and isotopic reactions can be applied to hot springs as geochemical thermometers to estimate subsurface reservoir temperatures. Geothermometers here applied to the Goddard System are: 1) silica (130°C), 2) quartz vs. pH (148°C), 3) quartz, assuming no steam loss (141°C), and 4) sodium/potassium (160°C).

The quartz geothermometer reportedly works well for hot spring water (Fournier, 1981). The calculations presented here are based on a model in which all of the silica is taken to be quartz (typically the case in granitic terranes) and in which there is no steam loss. The applicable formula (Fournier, 1981) is: temperature in centigrade = (1309/5.19-logC)-273.15, where C is the concentration of dissolved silica in ppm. This yields a value of 141°C. Another geothermometer, Na/K, has the advantage of being less affected by dilution and steam separation than other commonly used geothermometers (Fournier, 1981). Using the sodium and potassium concentrations in ppm in the formula: log (Na/K)=X, and plotting the result on the appropriate graph of Fournier (1981), yields a reservoir temperature of 160°C. Reservoir temperatures from the silica, and quartz vs. pH geothermometers were derived from plotting the values on graphs also developed by Fournier (1981).

Geochemical constraints on hot springs water source

The subsurface water source, on the basis of fluid geochemistry, is primarily a fresh one, however, a saline component must be present also. The springs have a high chloride, sodium and sulphate concentration relative to nearby streams and ground water, as well as other hot springs in southeastern Alaska. Redoubt Lake, a fresh water lake at

the surface, has a saline layer below 100 meters which is a potential source of ions for the hot springs system. Within this layer, dissolved solids are more abundant by a factor of 2 to 3 times relative to the upper fresh water layer (McCoy, 1977). Migration of some of this saline water a distance of 2.5 km to the hot springs site through the igneous and metamorphic bedrock is possible. Igneous and metamorphic rocks normally have a low primary permeability, however, a major lithologic contact, area fault-trends and a joint system trend parallel to the length of Redoubt Lake, and directly toward Goddard Hot Springs. Joints have a moderate secondary permeability and provide an avenue for groundwater migration. The chloride anion typically has a high mobility in ground water supporting its hypothesized migration from Redoubt Lake to the springs. Sodium, which constitutes 7000 ppm below 125 m in Redoubt Lake (McCoy,1977), and 1344 ppm in the Main Spring at Goddard would presumably be in combination with the chloride ion.

Isotope geochemistry

Variations in the oxygen-18/oxygen-16 and deuterium/hydrogen isotopic ratios of several components of geothermal fluids yield information about recharge areas and mixing phenomena between different fluids (Panichi and Gonfiantini, 1978). Geothermal fluids at Goddard Hot Springs are most similar in deuterium and oxygen-18 content to that of nearby cold water streams and non-saline water of Redoubt Lake (figure 23). This suggests that geothermal fluids are dominated by meteoric waters that are being heated during deep circulation. This interpretation is consistant with the work of Craig and others (1956) who showed that geothermal fluids are similar in deuterium content to local precipitation and Craig (1961) who determined the relationship of oxygen-18 to possible recharge areas.

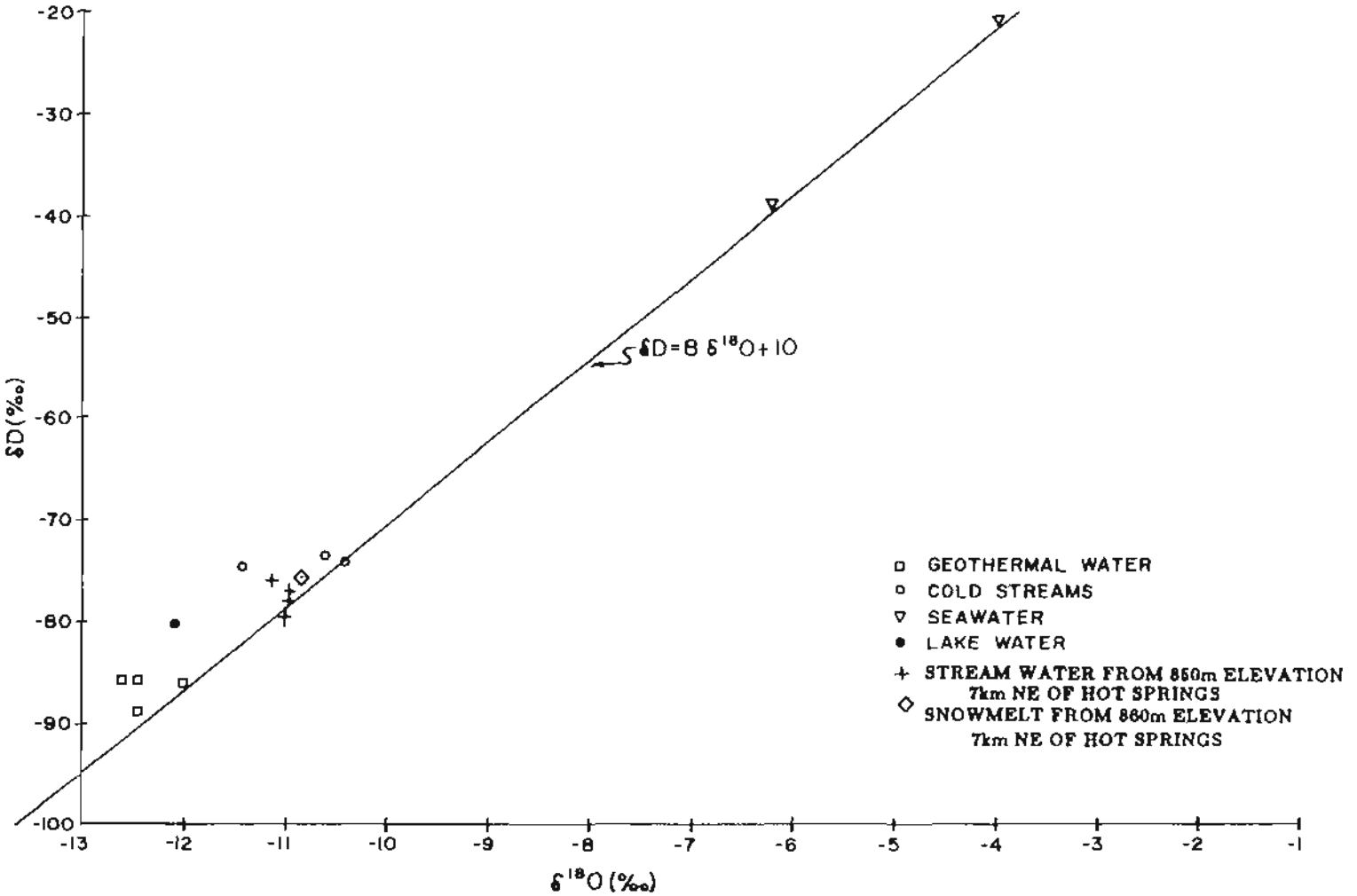

Figure 23. Deuterium and oxygen-18 compositions of geothermal fluid from the Goddard Hot Springs, area cold streams, near-by sea water and Redoubt Lake surface water. Diagonal line is the 'meteoric water line' of Craig(1961).

Oxygen isotopes in geothermal systems are exchanged between the hot rocks and deeply circulated meteoric waters. Typically this produces an oxygen isotope shift to higher oxygen-18 contents in the geothermal fluids. However, Truesdell and Hulson (1980) showed that systems with maximum reservoir temperatures below 150°C, moderate water/rock ratios and igneous rocks of an original oxygen-18 content of about +5 parts per mil may show little or no isotopic shift. The Goddard isotopic, geothermometry and petrographic data suggest such a system.

The isotopic composition of the Goddard thermal waters requires a source more depleted in deuterium and oxygen-18 than any of the surface waters sampled. Since deuterium and oxygen-18 are fractionated into condensed phases, precipitation farther inland and at higher altitude becomes progressively depleted in these heavy isotopes (Truesdell and Hulson, 1980). The altitude effect accounts for about 0.3 parts per mil decrease in oxygen-18 content and 2.5 parts per mil decrease for deuterium content per 100 m increase in elevation (Panichi and Gonfiantini, 1978). Using these values, meteoric waters from above a 500 m elevation should yield the heavy isotope signature indicated by the hot springs data. Within 2 km of the hot springs several peaks are over 800 m in elevation. Snow-melt and stream-headwaters were sampled for isotopic analyses 7 km NE of Goddard at the 850 m elevation. These analyses yield higher deuterium and oxygen isotopic values relative to the geothermal waters (figure 23) and to calculated values based on the expected heavy isotope altitude reduction.

On the basis of fifteen isotopic analyses of water from six different sources the high-elevation stream and Redoubt Lake samples yield the most isotope-depleted values. However, another heavy isotope-depleted source is required. That geothermal fluid recharge source is unidentified thus far but probably includes recharge from the Goddard area's higher elevations on western Baranof Island.

Interpretation

The Goddard system's peculiar fluid geochemistry and isotopic data requires a recharge component possibly from the saline layer of Redoubt Lake, or the ocean, or both. However, relatively low heavy isotope values for the hot springs preclude a saline source as the dominant reservoir recharging fluid. A geothermal mixing model which satisfies fluid geochemistry and the isotopic data is a system where groundwater, which originated as precipitation on the 1000 meter-high (or higher) mountains to the east, mixes with a smaller percentage of saline waters. If the reservoir system is less than 150°C no positive oxygen isotope shift will occur, and isotope mixing will be along the meteoric water line of Craig (1961). This model is consistent with the geothermometers of the geothermal fluids and the oxygen-18, deuterium, and fluid chemistry of the thermal fluids, cold-water streams and ocean water of the Goddard area.

Thermal transfer in the Goddard geothermal system is here interpreted to be of the water-dominated, convective heat transfer type of Rybach (1981). In convective systems the geothermal fluid loses heat to adjacent hydraulically connected rock, and naturally occurring convection transfers most of the heat (Gang and Kassoy, 1981). In contrast, the working fluid in conductive systems is either present, as in the deep aquifers in sedimentary basins, or must be supplied, as in the hot dry rock system (Rybach, 1981). In either of the conductive models above, an impermeable lithologic barrier exists between the upflow zone (from the deep hot reservoir) and the intersecting rocks. In the Goddard system such an impermeable barrier is not indicated on the basis of detailed bedrock geologic mapping of the springs area.

It is not entirely clear whether heating of the geothermal fluids in the Goddard system is due to: 1) a young igneous intrusion at some depth, or 2) deep circulation in an area of high to normal regional geothermal gradient- 42 to 25°C/km (Nathenson and others, 1983). However, the latter model is favored on the basis of: 1) southeastern Alaska's active tectonism, 2) the numerous faults on, and around, Baranof Island (these faults provide avenues for fluid migration), and 3) the isotopic and geothermometry data which suggest a relatively low temperature reservoir; one less likely to be a result of a hot igneous intrusion. The Mount Edgecumbe volcanic system erupted in Holocene time suggesting a high geothermal gradient in this vicinity.

The Goddard Hot Springs system is here interpreted to beof the liquid-dominated, warm water type of Donaldson and Grant (1981). One of the characteristics of this type of system is that during exploitation of the geothermal fluids no boiling is anticipated under any expected pressure drawdowns. On the basis of this classification and the distance from a population center, the Goddard geothermal system would best be utilized as a local energy source; exploited for agricultural purposes (including hydroponic farming), aquaculture development or home heating.

SUMMARY OF CONCLUSIONS

Detailed study of the Goddard Hot Springs area field geology, fluid geochemistry, petrography, and wholerock and isotope chemistry, data allow the following conclusions.

1) In light of Mutti and Ricci Lucchi's (1973) turbidite facies associations and environmental model, the Goddard area Sitka Graywacke represents inner fan and lower slope deposits.

2) The provenance terrane for these clastic rocks is a volcano-plutonic complex.

3) Predominant deformational style in the Sitka Graywacke is imbricate thrust faulting. Here, stratigraphic tops are to the northeast regardless of whether the beds are overturned. Imbricate thrust packets (Seely and others, 1974) are the typical structures of subduction and accretionary tectonics (Karig and Sharman, 1975).

4) Three gradational facies occur in the northwestern portion of the Crawfish Inlet pluton: 1) the centrally located tonalite facies, 2) the granodiorite facies, and 3) the primary white mica-bearing border facies.

5) Two petrogenetic models can account for the field, petrologic and chemical data bearing on the Crawfish Inlet pluton. In one model, an igneous body of tonalite bulk composition intrudes the flyschoid country rocks entraining large blocks. Anatexis along the pluton's border causes the bulk composition to become more siliceous and felsic (and locally peraluminous). A second model accounts for the chemical, mineralogical and fractionation changes through a particular magmatic evolution. Here, fractional crystallization of hornblende and timing and quantity of biotite crystallization controls whether late-stage magmatic evolution yields a peraluminous melt (Zen and Hammerstrom, 1983).

6) Data bearing on the alleged anatectic origin of the Crawfish Inlet pluton indicate a non-anatectic petrogenesis. Present data: modal mineralogy, major oxides, field

mapping, petrography, and Rb\Sr analyses indicate a primary magmatic origin, with only minor country rock assimilation.

7) The Crawfish Inlet pluton is anomalous relative to the anatectic plutons of the Sanak-Baranof belt of Hudson and others (1979), in that this pluton, almost invariably contains modal hornblende. Also, modal quartz, plagioclase and potassium feldspar compositions indicate more plagioclase and less quartz than modes for Sanak-Baranof plutons. Though these data sets overlap in part, the correlation is very poor. On the basis of these data, the Crawfish Inlet pluton is different from Sanak-Baranof-belt plutons and should not be included as part of the belt.

8) Sr and Rb data do not yield a reliable isochron. Initial 87Sr/86Sr ratios calculated using the 48.0 m.y. K-Ar age range from 0.70464 to 0.70527 and lie within the range for Phanerozoic orogenic batholiths. The magma has not interacted with an isotopic-rich crustal source but it's origin can not be exclusively defined. The preferred petrogenetic model is crustal contamination of a mantle-derived magma.

9) Contact metamorphic mineral assemblages indicate a pressure-temperature environment that ranges from 1 kb to more than 5 kb and from 525 to 650°C. The approximately 2 kb value based on an aplite dike of the Crawfish Inlet pluton is the preferred pressure value.

10) Subsurface temperatures for the Goddard geothermal system on the basis of four cation geothermometers range from 130 to 160°C. The absence of a positive oxygen isotope shift in the geothermal fluids is consistant with a reservoir temperature in this range (Truesdell and Hulson, 1980). Fluid recharge includes a heavy isotope-depleted one (high altitude ?), though this recharge component remains unidentified. Additional recharge is derived from the saline layer of Redoubt Lake, sea water, or both.

11) The Goddard system is the liquid-dominated warm water type of Donaldson and Grant (1981). Thermal transfer is the water-dominated, convective heat transfer type of Rybach (1981).

12) The Goddard system, if developed, would be best utilized as a local energy source (Sitka is 24 km to the north) and exploited for agricultural purposes (including hydroponic farming), aquaculture development or home heating.

13) Heating of the geothermal fluids is interpreted to be due to deep circulation in an area of high to normal regional geothermal gradient: 42 to 25°C/km.

REFERENCES CITED

Barker, Fred, 1979, Trondhjemite: definition, environment and hypotheses of origin, IN Trondjhemites, Dacites, and Related Rocks, Barker, Fred (Ed.): Elsevier Scientific Publishing Company, Amsterdam, The Netherlands, 659 p.

Bateman, P. C., Busacca, A. J. and Sawka, W. N., 1983, Cretaceous deformation in the western foothills of the Sierra Nevada California: Geological Society of America Bulletin, v. 94, p. 30-42.

Berg, H. C., and Hinckley, D. W., 1963, Reconnaissance geology of northern Baranof Island, Alaska: U. S. Geological Survey Bulletin 1141-0, p. 1-24.

Berg, H. C., Jones, D. L. and Coney, P. J., 1978, Map showing pre-Cenozoic tectonostratigraphic terranes of southeastern Alaska and adjacent areas: U. S. Geological Survey Open-File Report 78-1085, 2 sheets, scale 1:1,000,000.

Bliss, J. D., 1983, Alaska, basic data for thermal springs and wells as recorded in Geotherm: U. S. Geological Survey Open-File Report 83-426, 114 p.

Carmichael, I. S. E., Turner, F. J. and Verhoogen, J., 1974, Igneous petrology: McGraw-Hill, Inc., New York, 739 p.

Cowan, D. S., Geological evidence for post-40 m.y. B. P. large-scale northwestward displacement of part of southeastern Alaska: Geology, v. 10. p. 309-313.

Cox, K.G., Bell, J.D., and Pankhurst, R.J., 1979, The Interpretation of Igneous Rocks: George Allen & Unwin LTD., London, 450 p.

Craig, Harman, 1961, Isotopic variations in meteoric waters: Science, 133, p. 1702-1703.

Craig, Harman, Boato, Giovanni and White, D. E., 1956, Isotopic geochemistry of thermal waters: National Academy of Science Natural Resource Council, Publication 400, p. 29-38.

Deer, W. A., Howie, R. A. and Zussman, J., 1966, An introduction to the rock forming minerals: Longman, London, 528 p.

Decker, John, 1980, Geology of a Cretaceous subduction complex western Chichagof Island southeastern Alaska, Ph.D. dissertation: Stanford University, Stanford, California.

Donaldson, I. G. and Grant, M. A., 1981, Heat extraction from geothermal reservoirs in geothermal systems: Principles and case histories, Rybach, L., and Muffler, L. J. P. (Eds.), John Wiley and Sons Ltd., New York, p. 145-179.

Folk, R. L., 1974, Petrology of Sedimentary Rocks: Hemphill Publishing Company, Austin, Texas, 182 p.

Fournier, R. O., 1981, Application of water geochemistry to geothermal exploration and reservoir engineering, in Geothermal systems: Principles and case histories, Rybach, L. and Muffler, L. J. P. (Eds.): John Wiley and Sons Ltd., New York, p. 109-143.

Garg, S.K. and Kassoy, D. R., 1981, Convective heat and mass transfer in hydrothermal systems, in Geothermal systems: principles and case histories: Rybach, L., and Muffler, L. J. P. (Eds.): John Wiley and Sons Ltd., New York, p. 37-68.

Gehrels, G. E., Saleeby, J. B. and Berg, H. C., 1983, Preliminary description of the Late Silurian-Early Devonian Klakas Orogeny in the southern Alexander Terrane, southeastern Alaska, in Paleozoic and Early Mesozoic rocks in microplates in western North America: Pacific Section, Society of Economic Paleontologists and Mineralogists, Pacific Coast Paleogeography Symposium, Stephens, D. (Ed.): in press.

Hicks, S. D. and Shofnos, William, 1965, The determination of land emergence from sea level observations in southeast Alaska: Journal of Geophysical Research, v. 73, no. 2, p. 607-612.

Hudson, Travis, Plafker, George and Peterman, Z. E., 1979, Paleogene anatexis along the Gulf of Alaska margin: Geology, v. 7, no. 12, p. 573-577.

Hyndman, D. W., 1972, Petrology of igneous and metamorphic rocks: McGraw-Hill, Inc., New York, 533 p.

James, R. S. and Hamilton, D. L., 1969, Phase relations in the system NaAlSi3O8-KALSi3O8-CaAl2Si2O8-SiO2 at 1 kilobar water vapor pressure: Contributions to Mineralogy and Petrology, v. 21, p. 111-141.

Karig, D. E. and Sharman III, G. F., 1975, Subduction and accretion in trenches: Geological Society of America Bulletin, v. 86, p. 377-389.

Kosco, D. G., 1981, Part I: The Mt. Edgecumbe Volcanic field, Alaska: an example of tholeiitic and calc-alkaline volcanism, Part II: Characteristics of andesitic to dacitic volcanism dissertation: University of California, Berkeley, California, 249 p.

Loney, R. A., Berg, H. C., Pomeroy, J. S., and Brew, D. A., 1963, Reconnaissance geologic map of Chichagof Island and northwestern Baranof Island, Alaska: U. S. Geological Survey Miscellaneous Geologic Investigations, Map I-388, scale 1:250,000.

Loney, R. A., Brew, D. A. and Lanphere, M. A., 1967, Post Paleozoic radiometric ages and their relevance to fault movements, northern southeastern Alaska: Geological Society of America Bulletin, v. 78, p. 511-526.

Loney, R. A., Brew, D. A., Muffler, L. J., and Pomeroy, J. S., 1975, Reconnaissance geology of Chichagof, Baranof and Kruzof Islands, southeastern Alaska: U. S. Geological Survey Professional Paper No. 792, 105 p.

Luth, W. C., Jahns, R. H., and Tuttle, O. F., 1964, The granite system at pressures of 4 to 10 kilobars: Journal of Geophysical Research, volume 69,pp. 759-773.

McCoy, G. A., 1977, A reconnaissance investigation of a large meromictic lake in southeastern Alaska: Journal of Research, U. S. Geological Survey, v. 5, no. 3, May-June p. 319-324.

Miller, C. F. and Bradfish, L. J., 1980, An inner Cordilleran belt of muscovite-bearing plutons: Geology, v. 8, p. 412-416.

Miyashiro, Akiho, 1974, Volcanic rock series in island arcs and active continental margins: American Journal of Science, v. 274, p. 321-355.

Moore, J. C., 1973, Cretaceous continental margin sedimentation, southwestern Alaska: Geological Society of America Bulletin, v. 84, p. 595-614.

Motyka, R. J., Moorman, M. A. and Reeder, J. W., 1980, Assessment of thermal springs sites in southern southeastern Alaska - preliminary results and evaluation: Alaska Division of Geological and Geophysical Surveys, Alaska Open-File Report 127, 72 p.

Mutti, Emiliano and Ricci Lucchi, Franco, 1972, Le torbiditi dell'Appenino settentrionale-intodusione all'analisi de facies; Turbidites of the northern Apennines-introduction to facies analysis-with English summary: Memorie del la Societa Geologic Italiana, v. 11, p. 161-199.

Myers, J. D., 1980, Geology and petrology of the Edgecumbe volcanic field, southeastern, Alaska: Transform fault volcanism and magma mixing: Ph.D. dissertation, The Johns Hopkins University, Baltimore, Maryland.

Nathenson, Manuel, Guffanti, Marianne, Sass, J. H. and Monroe, R. M., 1983, Regional heat flow and temperature gradients, in Assessment of low-temperature geothermal resources of the United States-1982, Reed, M. J. (Ed.): U. S. Geological Survey, Geological Survey Circular 892, 73 p.

Nilsen, T. H., and Zuffa, G. G., 1982, The Chugach Terrane, a Cretaceous trench-fill deposit, southern Alaska, in Trench-Forearc Geology (Leggett, J. K., Ed.): Blackwell Scientific Publications, London, 576 p.

Page, Robert, 1973, The Sitka, Alaska earthquake of 1972 an unexpected visitor: Earthquake Information Bulletin, 5, no. 5, p. 4-9.

Panichi, C. and Gonfiantini, R. C., 1978, Environmental isotopes in geothermal studies: Geothermics, Vol. 6, p. 143-161.

Plafker, George, Jones, D. L. and Pessagno, E. A., Jr., 1977, A Cretaceous accretionary flysch and melange terrane along the Gulf of Alaska - accomplishments during 1976, Blean, K. M. (Ed.): U. S. Geological Survey Circular 751-B, p. B41-B43.

Presser, T. S., and Barnes, Ivan, 1974, Special techniques for determining chemical properties of geothermal waters: U.S. Geological Survey Water-Resources Investigation 22-74, 11 p.

Reineck, H. G. and Singh, I. B., 1980, Depositional sedimentary environments: Springer-Verlag, New York, 549 p.

Rybach, Ladislaus, 1981, Geothermal systems, conductive heat flow, geothermal anomalies, in Geothermal systems: principles and case histories, L. Rybach and L. J. P. Muffler (Eds.), 1981, John Wiley and Sons Ltd., New York, p. 3-31.

Rybach, Ladislaus and Muffler, L. J. P. (Eds.), 1981, Geothermal systems: principles and case histories: New York, John Wiley and Sons, 359 p.

Seely, D. R., Vail, P. R., and Walton, G. G., 1974, Trench slope model, IN The Geology of Continental Margins, Burk, C. A. and Drake, C. L. (Eds.): Springer-Verlag, New York, 1009 p.

Streckeisen, A. L., 1973, Plutonic rocks, Classification and nomenclature recommended by the IUGS subcommission on the systematics of igneous rocks: Geotimes, Oct., p. 26-30.

Swanson, S. E., 1978, Petrology of the Rocklin pluton and associated rocks, western Sierra Nevada, California: Geological Society of America Bulletin, v. 89, p. 679-686.

Tocher, Don and Miller, D. J., 1959, Field observations on effects of Alaska earthquake of 10 July 1958: Science, v. 129, no. 3346, p. 394-395.

Truesdell, A. H. and Hulson, J. R., 1980, Isotopic evidence on environments of geothermal systems, in Handbook of environmental isotope geochemistry, Fritz, R., and Fontes, J. Ch., (Eds.): Elsevier Scientific Publishing Company, Amsterdam, The Netherlands, p. 179-226.

Turner, F. J., 1981, Metamorphic petrology: mineralogical, field and tectonic aspects: McGraw-Hill, Inc., New York, 533 p.

Tuttle, O. F. and Bowen, N. L., 1958, Origin of granite in the light of experimental studies in the system $NaAlSi_3O_8$-$KAlSi_3O_8$-SiO_2-H_2O: Geological Society of America Memior 74, 153 p.

Twenhofel, W. S. and Sainsbury, C. L., 1958, Fault patterns in southeastern Alaska: Geol. Soc. America Bull., v. 69, p. 1431-1442.

van der Plas, L. and Tobi, A. C., 1965, A chart for judging the reliability of point counting results: American Journal of Science, v. 263, p. 87-90.

von Huene, Roland, Fisher, M. A. and Bruns, T. R., 1977, Continental margins of the Gulf of Alaska and late Cenozoic tectonic plate boundaries, in Alaska Geological Society, 1977, symposium proceedings, J1-33.

Walker, R. G. and Mutti, Emiliano, 1973, Turbidite facies and facies associations, in Paleontologists and Mineralogists, Pacific section, Middleton, G. V., and Bouma, A. H., (co-chairmen), Lecture Notes for Short Course, p. 119-157

Waring, G. A., 1917, Mineral springs of Alaska: U. S. Geological Survey Water-Supply Paper 418, 118 p.

Westbrook, G. K. and Smith, M. J., 1983, Long decollements and mud volcanoes: Evidence from the Barbados Ridge Complex for the role of high pore-fluid pressure in the development of an accretionary complex: Geology, v. 11, p. 279-283.

Winkler, H. G. F., 1979, Petrogenesis of metamorphic rocks, fifth edition: Springer, New York, 348 p.

Zen, E-an, and Hammerstrom, J. M., 1983, Mineral chemistry and fractionation trends exemplified by a pluton from the Pioneer batholith, southwest Montana: Geological Society of America, Abstract with programs, 1983: Geological Society of America, volume 15, number 6, p. 726.

Zuffa, G. G., Nilsen, T. H. and Winkler, G. R., 1980, Rock-fragment petrography of the Upper Cretaceous Chugach terrane, southern Alaska: U. S. Geological Survey Open-File Report 80-713, 27 p.

APPENDIX 1

WHOLE ROCK MAJOR OXIDE AND CIPW NORM DATA FOR SOME ROCKS OF THE THE GODDARD AREA.*

	Sandstone & shale	Hornfelsed shale	Greenstones		
	81RR004	81RR316	81RR373	81RR374	81RR377
SiO2	65.18	65.97	46.76	59.97	47.16
Al2O3	14.30	16.47	17.01	18.56	17.27
Fe2O3	1.03	1.17	2.91	1.40	1.38
FeO	3.88	3.60	7.58	5.12	9.68
MgO	2.56	2.03	3.45	2.75	5.35
CaO	2.87	1.67	8.46	1.73	8.23
Na2O	3.07	2.41	3.52	2.19	3.44
K2O	1.86	3.00	0.67	3.60	1.07
TiO2	0.69	0.58	1.57	0.84	1.76
P2O5	0.19	0.14	0.35	0.19	0.37
MnO	0.09	0.10	0.21	0.20	0.19
LOI	2.38	2.53	5.32	3.18	1.99
H2O	0.46	0.24	0.23	0.25	0.18
Total	98.56	99.91	98.04	99.98	98.07
Q			-	23.70	-
C			-	8.67	-
Or			4.25	22.04	6.62
Ab			32.24	19.21	30.38
An			30.95	7.57	29.72
Lc			-	-	-
Ne			-	-	-
Di			9.92	-	8.54
Wo			4.99	-	4.30
Hy			12.69	14.59	1.29
Ol			1.29	-	16.99
Mt			4.57	2.10	2.09
Il			3.23	1.65	3.49
Ap			0.88	0.46	0.90
Cc			-	-	-

APPENDIX 1 continued

	Xenoliths			Hornblende hornfels	
	81RR196	81RR309	81RR379I	81RR224	81RR236
SiO2	66.57	70.54	66.87	61.33	52.80
Al2O3	14.77	14.12	14.37	17.39	18.67
Fe2O3	0.83	0.90	0.77	0.95	1.74
FeO	3.37	3.09	3.35	5.94	7.80
MgO	1.94	1.31	1.86	2.64	3.16
CaO	2.73	1.62	3.64	2.10	6.21
Na2O	3.57	3.18	3.63	2.61	5.61
K2O	2.91	3.22	1.97	2.82	1.21
TiO2	0.56	0.47	0.57	0.82	1.73
P2O5	0.15	0.07	0.16	0.50	0.17
MnO	0.08	0.09	0.07	0.10	0.18
LOI	0.57	0.78	1.19	1.92	1.16
H2O	0.26	0.19	0.22	0.47	0.27
Total	98.31	99.58	98.67	99.59	100.71
Q	24.80	33.00	26.68	24.92	-
C	1.16	2.67	0.02	7.62	-
Or	17.67	19.32	12.00	17.14	7.15
Ab	30.97	27.25	31.56	22.76	44.87
An	12.91	7.68	17.51	7.38	22.19
Lc	-	-	-	-	-
Ne	-	-	-	-	-
Di	-	-	-	-	11.19
Wo	-	-	-	-	3.14
Hy	9.82	7.68	9.58	15.98	-
Ol	-	-	-	-	-
Mt	1.23	1.32	1.15	1.42	2.52
Il	1.08	0.91	1.12	1.60	3.29
Ap	0.35	0.16	0.37	1.18	0.39
Cc	-	-	-	-	-

	Hypabyssal dikes				Aplite dike
	81RR010	81RR297	81RR375	81RR153	81RR051
SiO2	46.86	46.73	49.56	46.20	71.59
Al2O3	16.30	16.97	17.49	16.34	13.67
Fe2O3	2.14	2.59	2.76	3.74	0.08
FeO	9.29	6.54	7.54	6.66	1.76
MgO	6.27	8.47	3.70	8.69	0.57
CaO	9.73	10.63	6.99	10.05	2.10
Na2O	3.63	3.46	4.93	3.01	3.82
K2O	0.39	0.41	1.26	0.21	3.48
TiO2	2.02	1.17	2.11	1.24	0.22
P2O5	0.33	0.13	0.20	0.16	0.13
MnO	0.21	0.16	0.17	0.18	0.05
LOI	0.81	2.65	2.01	1.67	0.51
H2O	0.54	0.53	0.23	1.04	0.29
Total	98.52	100.44	98.95	99.19	98.27
Q	-	-	-	-	30.53
C	-	-	-	-	0.11
Or	2.36	2.48	7.68	1.30	21.10
Ab	29.12	23.02	39.13	26.40	33.17
An	27.79	30.39	22.60	31.57	9.82
Lc	-	-	-	-	-
Ne	1.37	3.85	2.18	-	-
Di	16.19	18.48	9.81	15.25	-
Wo	8.23	9.60	4.97	7.94	-
Hy	-	-	-	2.27	4.42
Ol	15.25	15.33	9.85	14.77	-
Mt	3.19	3.86	4.13	5.63	0.12
Il	3.95	2.28	4.14	2.45	0.44
Ap	0.76	0.30	0.49	0.39	0.30
Cc	-	-	-	-	-

APPENDIX 1 continued

	Plutonic rocks				
	Border facies				
	81RR030	81RR034	81RR080	81RR142	81RR165
SiO2	68.19	72.66	63.16	72.86	67.20
Al2O3	15.67	13.44	16.43	13.80	16.59
Fe2O3	0.42	0.03	0.83	0.02	0.47
FeO	2.37	1.71	3.84	1.67	2.79
MgO	1.02	0.54	1.86	0.36	16
CaO	4.01	1.97	4.65	1.53	4.14
Na2O	4.08	3.73	3.77	3.86	4.06
K2O	1.99	3.68	2.22	4.31	1.82
TiO2	0.45	0.22	0.70	0.14	0.47
P2O5	0.12	0.10	0.15	0.08	0.29
MnO	0.05	0.04	0.09	0.05	0.07
LOI	0.25	0.21	0.48	0.23	0.46
H2O	0.29	0.29	0.41	0.35	0.24
Total	98.91	98.62	98.59	99.26	99.96
Q	26.07	31.45	18.57	29.39	24.87
C	-	-	-	0.19	1.11
Or	11.94	22.16	13.41	25.82	10.81
Ab	35.12	32.15	32.66	33.09	34.61
An	18.87	9.25	21.86	7.17	18.79
Lc	-	-	-	-	-
Ne	-	-	-	-	-
Di	0.49	0.06	0.64	-	-
Wo	0.24	0.03	0.32	-	-
Hy	5.75	4.22	9.91	3.85	7.54
Ol	-	-	-	-	-
Mt	0.62	0.04	1.23	0.03	0.68
Il	0.87	0.42	1.37	0.27	0.89
Ap	0.28	0.23	0.35	0.19	0.67
Cc	-	-	-	-	-

APPENDIX 1 continued

	Plutonic rocks				
	Border facies				
	81RR187	81RR193	81RR227	81RR279	81RR281
SiO2	61.89	60.53	66.60	73.82	68.61
Al2O3	17.18	17.41	16.08	13.62	14.94
Fe2O3	0.87	0.73	0.61	0.02	0.50
FeO	4.16	4.09	3.26	1.12	2.36
MgO	2.91	2.13	1.25	0.43	1.33
CaO	5.34	5.24	3.90	2.17	3.43
Na2O	3.64	4.00	4.28	3.99	3.91
K2O	1.74	1.94	1.71	3.52	2.88
TiO2	0.67	0.66	0.52	0.13	0.44
P2O5	0.16	0.16	0.16	0.08	0.09
MnO	0.10	0.09	0.09	0.04	0.06
LOI	0.50	1.03	0.29	0.53	0.43
H2O	0.27	0.27	0.30	0.24	0.19
Total	99.43	98.28	99.05	99.71	99.17
Q	16.23	13.83	23.54	31.51	25.00
C	-	-	0.47	-	-
Or	10.40	11.82	10.28	20.80	17.26
Ab	31.22	34.86	36.81	33.76	33.59
An	25.74	24.58	18.60	8.86	14.92
Lc	-	-	-	-	-
Ne	-	-	-	-	-
Di	0.04	0.97	-	1.17	1.45
Wo	0.02	0.49	-	0.58	0.73
Hy	13.41	11.17	8.02	2.38	5.98
Ol	-	-	-	-	-
Mt	1.28	1.09	0.90	0.03	0.74
Il	1.29	1.29	1.01	0.25	0.85
Ap	0.37	0.37	0.37	0.19	0.21
Cc	-	-	-	-	-

APPENDIX 1 continued

	Plutonic rocks				
	Border facies		Granodiorite facies		Tonalite facies
	81RR340	81RR378	81RR152	81RR156	81RR170
SiO2	61.63	62.92	68.50	67.43	65.05
Al2O3	16.50	16.17	14.99	15.00	16.00
Fe2O3	1.97	0.49	0.30	0.03	1.57
FeO	3.31	3.70	2.44	2.53	2.27
Mg	2.52	1.60	1.21	1.25	1.67
CaO	4.48	4.15	3.33	3.50	4.61
Na2O	3.37	3.79	4.07	3.81	3.99
K2O	1.35	2.46	2.74	3.07	1.86
TiO2	0.65	0.60	0.35	0.34	0.48
P2O5	0.18	0.16	0.10	0.11	0.15
MnO	0.11	0.07	0.07	0.06	0.08
LOI	2.23	1.78	0.51	0.57	0.39
H2O	0.31	0.18	0.34	0.30	0.30
Total	98.61	98.07	98.95	98.00	98.42
Q	23.29	18.88	24.73	23.67	22.65
C	1.85	0.12	-	-	-
Or	8.33	15.13	16.49	18.67	11.23
Ab	29.70	33.34	35.12	33.17	34.52
An	21.88	20.32	14.85	15.20	20.74
Lc	-	-	-	-	-
Ne	-	-	-	-	-
Di	-	-	1.09	1.62	1.37
Wo	-	-	0.55	0.81	0.71
Hy	10.25	9.89	6.37	6.69	5.86
Ol	-	-	-	-	-
Mt	2.97	0.74	0.45	0.04	2.33
Il	1.29	1.18	0.68	0.66	0.93
Ap	0.44	0.39	0.23	0.25	0.35
Cc	-	-	-	-	-

APPENDIX 1 continued

	Plutonic rocks				
	Tonalite facies				
	81RR173	81RR353	81RR363	81RR368	81RR372
SiO2	68.17	69.20	65.36	65.00	67.20
Al2O3	15.62	15.15	16.47	15.48	15.54
Fe2O3	0.62	0.43	0.78	0.97	0.47
FeO	2.62	2.10	2.88	3.27	2.53
MgO	1.57	1.15	1.64	1.88	1.38
CaO	3.95	3.44	3.90	4.02	4.08
Na2O	3.96	4.02	4.15	3.67	4.24
K2O	2.22	2.53	2.23	2.46	2.22
TiO2	0.42	0.34	0.45	0.56	0.41
P2O5	0.13	0.12	0.15	0.14	0.11
MnO	0.07	0.06	0.07	0.08	0.07
LOI	0.26	0.46	0.99	0.70	0.45
H2O	0.38	0.17	0.17	0.11	0.08
Total	99.99	99.17	99.24	98.34	98.78
Q	24.75	26.48	20.48	21.87	22.83
C	-	-	0.50	-	-
Or	13.18	15.19	13.18	14.89	13.35
Ab	33.76	34.52	35.11	31.82	36.55
An	18.40	16.03	18.37	18.98	17.10
Lc	-	-	-	-	-
Ne	-	-	-	-	-
Di	0.41	0.41		0.45	2.30
Wo	0.21	0.21		0.23	1.16
Hy	7.50	5.79	8.12	9.13	6.12
Ol	-	-	-	-	-
Mt	0.90	0.64	1.13	1.44	0.70
Il	0.80	0.66	0.86	1.08	0.80
Ap	0.30	0.28	0.35	0.32	0.25
Cc	-	-	-	-	-

*Analyses by X-ray fluorescence, DGGS Minerals Laboratory
LOI = Loss on ignition